

**EVALUATING UNCERTAINTY IN THE VOLUMES OF FLUIDS
IN PLACE IN AN OFFSHORE NIGER DELTA FIELD**

ENAWORU EFEOGHENE

**EVALUATING UNCERTAINTY IN THE VOLUMES OF FLUIDS
IN PLACE IN AN OFFSHORE NIGER DELTA FIELD**

By

Efeoghene Enaworu

RECOMMENDED:

Prof. (Emeritus) David O. Ogbe – Committee Chair

Prof. Samuel Osisanya – Committee Member

Dr. Alpheus Igbokoyi – Committee Member

APPROVED:

Chair, Department of Petroleum Engineering

Academic Provost

Date

EVALUATING UNCERTAINTY IN THE VOLUMES OF FLUIDS IN PLACE IN AN OFFSHORE NIGER DELTA FIELD

A THESIS

*Presented to the Graduate Faculty
Of African University of Science and Technology*

*In Partial Fulfilment of the Requirements
For the Degree of*

Master of Science in Petroleum Engineering

By

Enaworu Efeoghene, B.Sc.

Abuja, Nigeria

December, 2011

ABSTRACT

The purpose of this work is to evaluate the uncertainty in the volumes of fluids in place in Fault Block A (Segment 3) of the G-1 Sands in the OND field located offshore Niger Delta. The evaluation was performed in three parts: (1) building of the static model and division into three hydrocarbon zones with reference to the oil-water-contact (OWC); (2) estimating the distribution of petrophysical properties such as porosity, water saturation and net-to-gross ratio in the reservoir and; (3) generation of various realizations of the volumes of fluids in place (STOOIP) and evaluation of uncertainty of STOOIP in the OND field.

The first part was executed by building a grid-based model of the reservoir using eclipse and Petrel. A 100 x 60 x 4 grid was built and the faults were created in the model to delineate the reservoir into six segments. The second part of the study involved the calculation of the petrophysical properties that affect the volumes of fluids in place and distributing them in the geologic model. This was done by assigning various probability distribution functions to porosity, water saturation and net-to-gross; and calculating STOOIP for the three hydrocarbon zones using the method of Monte Carlo simulation. One hundred realizations of STOOIP were generated for each zone in the reservoir.

In the third part of the study the estimates of STOOIP for each zone were plotted as histograms to determine the P10, P50 and P90 values of STOOIP and these yardsticks were used to evaluate the uncertainty of the volumes of fluids in place (STOOIP) in the Fault Block A of the G-1 Sands in the OND field. The results of the study show that there is a general decrease in P10, P50 and P90 values for each zone with increase in depth. The proposed methodology of this work can be applied to other reservoirs for proper planning and field development.

DEDICATION

To the Lord God Almighty who gave me the opportunity and grace to become a Petroleum Engineer.

To my lovely wife Oghenetejiri, the love of my life. Who helped, stood by me and was patient with me throughout my studies and in making this work a huge success. You are indeed a blessing to me.

Muah!

ACKNOWLEDGEMENTS

Firstly, I give my greatest thanks, praise and honour to my heavenly Father for His Mercies Grace, Love, Care, Protection, Discipline, Provision, Guidance and Faithfulness towards me during the course of this thesis work. I love you very much Lord Jesus Christ.

I acknowledge the Department of Petroleum Engineering for Providing the @Risk, Eclipse and Petrel softwares.

I also want to thank my supervisor Prof. David O. Ogbe for his supervisory role and for making this thesis a knowledgeable and successful one. The Petroleum Engineering Co-ordinator – Professor Godwin Chukwu, for his fatherly role and making the MSc programme a success. To my committee members – Dr. Alpheus Ibkoyi and Dr. Samuel Osisanya, I say a big thank you for a job well done. For other various faculties who taught me and impacted their respective knowledge on me, I say a very big thank you to you all. I am sincerely privileged and forever grateful.

Words cannot express my gratitude to my lovely, unique, God fearing wife for being a blessing to me. I love you very much.

My sincere and heartfelt gratitude goes to my friends and colleagues – Biyi, Tunde, Joseph, Shaibu, Salasi, Oscar, Ayefu, Bayo, Johnson, Harrison, Emmanuel, Ohinuwa, Olem, Charles, Omotayo, Phillip, George, Vodah, Bimpe, Lowestein and Ene, God bless you all.

TABLE OF CONTENTS

Contents	Page
Signature Page.....	ii
Title Page	iii
Abstract.....	iv
Dedication.....	v
Acknowledgements.....	vi
Table of contents.....	vii
List of Figures.....	x
List of Tables.....	xii
List of Appendice.....	xiii
 CHAPTER ONE	
1.0 INTRODUCTION.....	1
1.1 Study Objectives.....	3
1.2 Scope of Study.....	3
 CHAPTER TWO	
2.0 LITERATURE REVIEW.....	4
2.1 Review of the Geology of the Niger Delta.....	4
2.1.1 Review of the Stratigraphy.....	7

2.1.2	Review of the Hydrocarbon Occurrence.....	11
2.2	Overview of the Meren Field.....	13
2.2.1	Geology and Reservoir Characteristics.....	16
2.2.2	Occurrence of Hydrocarbon.....	18
2.2.3	Rock Properties.....	21
2.2.4	Rock Sensitivity.....	21
2.3	Overview of Uncertainty Evaluation.....	22
2.3.1	Uncertainty Evaluation in Oil in Place Volumes.....	25
2.3.2	Uncertainty Evaluation in Gas In Place Volumes.....	26
2.3.3	Uncertainty Evaluation in Forecasting Rate and Production Efficiency.....	26
2.3.4	Impacts on Uncertainty in Static and Dynamic Modeling.....	27
2.4	Overview of Various Methodologies of Accounting for Uncertainties.....	27
2.4.1	Limitations and Shortcomings of Some Existing Uncertainty Methods.....	28

CHAPTER THREE

3.0	METHODOLOGY.....	30
3.1	Geological Modeling.....	30
3.1.1	Horizon and Zone Modeling.....	32
3.1.2	Fault Modeling.....	32
3.2	Petrophysical Modeling.....	33
3.2.1	Porosity.....	34
3.2.2	Net-To-Gross Thickness Ratio.....	35
3.2.3	Water Saturation.....	36
3.3	Uncertainty Evaluation of Volumes of Fluids in Place (STOOIP).....	37

CHAPTER FOUR

4.0 DISCUSSION OF RESULTS.....38
4.1 STOOIP for Zone 1.....39
4.2 STOOIP for Zone 2.....40
4.3 STOOIP for Zone 3.....40
4.4 Pertinent Remarks.....41

CHAPTER FIVE

5.0 CONCLUSIONS AND RECOMMENDATION.....42
5.1 Conclusion.....42
5.2 Recommendation.....42

REFERENCES.....44

APPENDIX A: NOMENCLATURE AND ABBREVIATIONS52

APPENDIX B: MODEL GRID FILE.....53

APPENDIX C: FAULT CODE FILE.....55

APPENDIX D: ADDITIONAL FIGURES FOR CHAPTER THREE62

APPENDIX E: ADDITIONAL FIGURES FOR CHAPTER FOUR.....66

LIST OF FIGURES

Figure	Page
2.1: Niger Delta Field Structures and Associated Traps.....	7
2.2: Stratigraphic Column Showing Formations of the Niger Delta.....	8
2.3: Location of Meren Field Offshore Nigeria.....	14
2.4: Scanning Electron Microscope (SEM) Photos.....	16
2.5: Sand G1 Structure Map.....	17
2.6: Sand G1 Isoporosity Map.....	18
2.7: Hydrocarbon Content in Fault Blocks A, B, and F.....	19
2.8: Relation of Porosity to Clay Content.....	21
3.1: Basic Workflow Used in the Gridbased Geologic Modeling & Uncertainty Evaluation.....	31
3.2: Grid Model Showing Fault Zones.....	32
3.3: Assignment of Probability Distribution.....	33
3.4: Uncertainty Sampling Method for Porosity.....	34
3.5: Example Realization of Porosity.....	35
3.6: Example Realization of Net-to-Gross Thickness Ratio.....	36
3.7: Example Realization of Water Saturation.....	36
4.1: Histogram Plot of STOOIP for Zone 1.....	39

4.2:	Histogram Plot of STOOIP for Zone 2.....	40
4.3:	Histogram Plot of STOOIP for Zone 3.....	41

LIST OF TABLES

Table		Page
2.1:	Formations of the Niger Delta Area	10
2.2:	Reservoir Properties and Production Summary.....	20
4.1:	STOOIP of Fault Block A of the G-1 Sands in MMSTB.....	39

LIST OF APPENDICE

Appendice	Page
APPENDIX A: Nomenclature and Abbreviations.....	52
APPENDIX B: Model Grid File.....	53
APPENDIX C: Fault Code File.....	55
APPENDIX D: Additional Figures for Chapter Three	62
Figure D1: G-1 Sands Isopach Map.....	62
Figure D2: G-1 Sands Gridded Isopach Map.....	62
Figure D3a: Model Showing Areal View of Grid Cells.....	63
Figure D3b: Model Showing Areal View of Grid Cells for Segment 3.....	63
Figure D4: Grid Model Showing Fault Zones.....	64
Figure D5: 3D Grid Model Showing Segments.....	64
Figure D6: 3D Grid Model Showing Grid Zones.....	65
APPENDIX E: ADDITIONAL FIGURES FOR CHAPTER FOUR	66
Figure E1: Uncertainty Evaluation of STOOIP for all Zones.....	68

CHAPTER ONE

1.0 INTRODUCTION

Reservoir Characterization is a process of integrating various qualities and quantities of data in a consistent manner to describe reservoir properties of interest in inter well locations (Ezekwe and Filler, 2005). The main purpose of reservoir characterization is to generate a more representative geologic model of the reservoir properties. More so, the goal of any reservoir characterization or reservoir modeling is to understand the reservoir connectivity in static and dynamic conditions by integrating data from different sources (Mondal, 2010). Thus, in building a Geologic representation of what a reservoir is most likely to be, it is necessary to adequately capture the uncertainty associated with not knowing its exact picture (Odai and Ogbe, 2010).

The success of any hydrocarbon exploration and exploitation program depends on the building of a reliable reservoir model. Furthermore, a reservoir's commercial life begins with exploration that leads to discovery, followed by characterization of the reservoir. However, the main challenge in reservoir development is the availability of limited data and huge uncertainty. Thus, this makes the evaluation of reservoir uncertainty very important in achieving a good understanding of reservoir management risks. Hence, the use of a practical method for estimating uncertainty without compromising accuracy is therefore clearly needed.

Petroleum resources also represent a significant part of a company's upstream asset and are the foundation of its current and future upstream activities. Often times, at the discovery of a new field or extension of an existing field, there are uncertainties associated with quantifying the amount of hydrocarbons in place (Akinwunmi *et al.*, 2004). These uncertainties may be related to

the structure, aerial extent of the accumulation, unseen fluid contacts to delineate the vertical extent, internal architecture of the reservoir and the characteristics of the resident fluids. Consequently, this has made it a routine in field development planning, to identify and quantify the impact of major subsurface uncertainties such as the hydrocarbon in-place volumes and their distribution (Akinwunmi *et al.*, 2004).

Other uncertainties encountered in reservoir engineering models as listed by Akaeze *et al.* (2004), includes: drive mechanism, permeability, aquifer support, fluid properties, reservoir extent and connectivity, end point saturations and reservoir structure. Subsequently, evaluating uncertainty using conventional methods, where model parameters are changed individually, makes it impossible to establish an objective business decision without underestimating the effects of uncertainty. Thus, decision making in the face of uncertainty becomes a problem which is usually encountered at every strategic level within the exploration and production value chain. Also, this problem is obvious in new field development projects when there is limited and uncertain geologic and engineering data. As such, it becomes pertinent to develop a systematic methodology for accounting for uncertainty during reservoir characterization and reservoir modeling in an offshore field.

The OND (offshore Niger Delta) field which will be our case study is loosely patterned after the Meren field, located on the Western edge of the Niger River Delta about 110 miles South-East of Lagos. It lies about 8 Miles offshore in approximately 40 feet of water (Thakur *et al.*, 1992) consisting of interstratified sandstones and shales, mostly representing shore face to shelf deposition (Cook *et al.*, 1999). According to Lumley *et al.* (2000), there are six major fault

blocks in the OND field, with each block containing dozen reservoir sands with more than 40 total producing sands.

1.1 STUDY OBJECTIVES

The overall objectives of this study are:

- To develop a methodology for evaluating uncertainty in STOOIP.
- To validate this methodology using a case study from an offshore OND field in the Niger Delta.
- To evaluate the uncertainty in the volumes of fluids in place (STOOIP) in the OND field.

1.2 SCOPE OF STUDY

This study is focused on an offshore Niger Delta field and entails the building of a geologic model using the Petrel¹ software tool. Various realizations of STOOIP will be generated for the zones in the reservoir model and uncertainty evaluated for each zone. The data from these realizations will be used in Monte Carlo simulations. Finally, the development of a systematic methodology for accounting for uncertainty in reservoir characterization and reservoir modeling will be discussed.

¹ Petrel is developed by Schlumberger

CHAPTER TWO

2.0 LITERATURE REVIEW

Introduction

The OND field in the shallow offshore Niger Delta Basin is the main focus area in this present study. A brief review of the Niger Delta basin tectonics, sedimentology and tertiary stratigraphy are important and necessary for readers to follow the rest of this thesis. The engineering studies, sequence stratigraphy, geology and reservoir characteristics of the OND field are also discussed below. An overview of various methodologies presented in the literature for accounting for uncertainty in STOOIP is highlighted.

2.1 Review of the Geology of the Niger Delta.

The Niger Delta clastic wedge formed along a failed arm of a triple junction system (aulacogen) that originally developed during the breakup of the South American and African plates in the late Jurassic (Burke *et al.*, 1972 and Whiteman, 1982). The two arms that followed the Southwestern and Southeastern coast of Nigeria and Cameroon developed into the passive continental margin of West Africa, whereas the third failed arm formed the Benue Trough. Other depocenters along the African Atlantic coast also contributed to the deltaic build-ups (Figure 2). Synrift sediments accumulated during the Cretaceous to Tertiary, with the oldest dated sediments of Albian age. Thickest successions of syn-rift marine and marginal marine clastics and carbonates were deposited in a series of transgressive and regressive phases (Doust and Omatsola, 1989).

The Synrift phase ended with basin inversion in the Santonian (Late Cretaceous). Renewed subsidence occurred as the continents separated and the sea transgressed the Benue Trough. The Niger Delta clastic wedge continued to prograde during Middle Cretaceous time into a

depocenter located above the collapsed continental margin at the site of the triple junction. Sediment supply was mainly along drainage systems that followed two failed rift arms, the Benue and Bida Basins. Sediment progradation was interrupted by episodic transgressions during Late Cretaceous time (Short and Stauble, 1967).

During the Tertiary, sediment supply was mainly from the north and east through the Niger, Benue and Cross Rivers. The Benue and Cross Rivers provided substantial amounts of volcanic detritus from the Cameroon volcanic zone beginning in the Miocene. The Niger Delta clastic wedge prograded into the Gulf of Guinea at a steadily increasing rate in response to the evolution of these drainage areas and continued basement subsidence. Regression rates increased in the Eocene, with an increasing volume of sediments accumulated since the Oligocene (Short and Stauble, 1967).

The morphology of Niger Delta changed from an early stage spanning the Paleocene to early Eocene to a later stage of delta development in Miocene time. The early coastlines were concave to the sea and the distributions of deposits were strongly influenced by basement topography (Doust and Omatsola, 1989). Delta progradation occurred along two major axes, the first paralleled the Niger River, where sediment supply exceeded subsidence rate. The Second, smaller than the first, became active during Eocene to early Oligocene basin ward of the Cross River where shorelines advanced into the Olumbe-1 area (Short and Stauble, 1967). This axis of deposition was separated from the main Niger Delta deposits by the Ihuo Embayment, which was later rapidly filled by advancing deposits of the Cross River and other local rivers (Short and Stauble, 1967).

Late stages of deposition began in the early to middle Miocene, as these separate Eastern and Western depocenters merged. In Late Miocene the delta prograded far enough that shorelines became broadly concave into the basin. Accelerated loading by this rapid delta progradation mobilized underlying unstable shales. These shales rose into diapiric walls and swells, deforming overlying strata (Short and Stauble, 1967).

According to Short and Stauble (1967) and Doust and Omatsola (1990), three major depositional cycles have been identified within Tertiary Niger Delta deposits. The first two, involving mainly marine deposition, began with a middle Cretaceous marine incursion and ended in a major Paleocene marine transgression. The second of these two cycles, starting in late Paleocene to Eocene time, reflects the progradation of a “true” delta, with an arcuate, wave- and tide-dominated coastline. These sediments range in age from Eocene in the north to Quaternary in the south (Doust and Omatsola, 1990). Deposits of the last depositional cycle have been divided into a series of six depobelts (Doust and Omatsola, 1990) also called depocenters or megasequences separated by major synsedimentary fault zones. These depobelts formed when paths of sediment supply were restricted by patterns of structural deformation, focusing sediment accumulation into restricted areas on the delta. Such depobelts changed position over time as local accommodation was filled and the locus of deposition shifted basin ward (Doust and Omatsola, 1990).

Normal faults triggered by the movement of deep-seated, over pressured, ductile, marine shale have deformed much of the Niger Delta clastic wedge (Doust and Omatsola, 1989). Many of these faults formed during delta progradation and were syndepositional, affecting sediment dispersal. In addition, these fault growths were also accompanied by slope instability along the

continental margin. Furthermore, faults flatten with depth onto a master detachment plane near the top of the over-pressured marine shales at the base of the Niger Delta succession. Thus, structural complexity in local areas reflects the density and style of faulting and simple structures, such as flank and crestal folds, occur along individual faults.

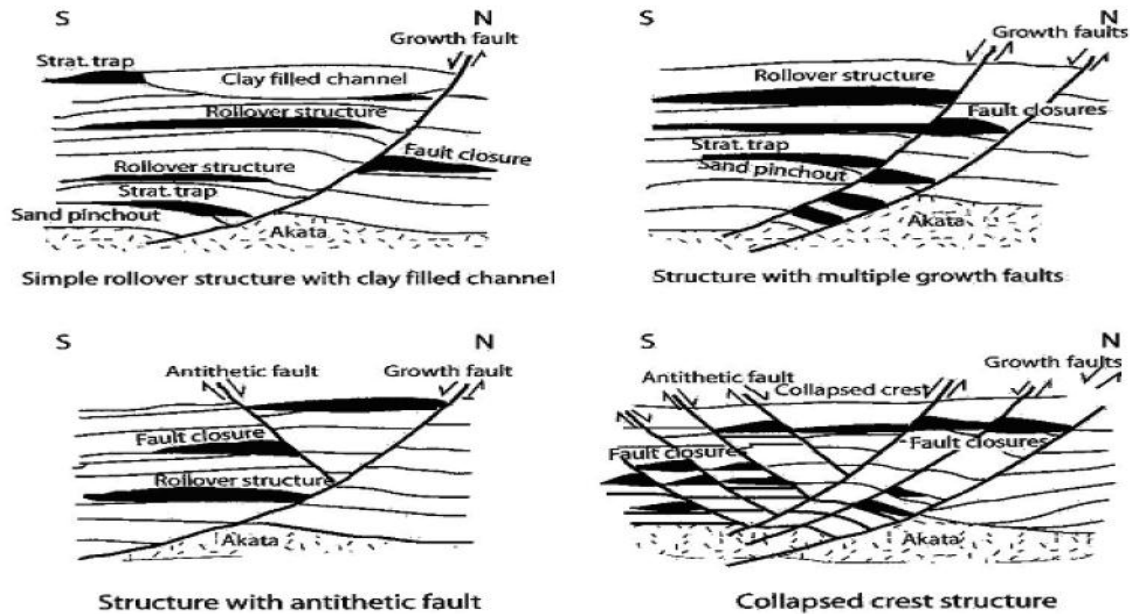


Figure 2.1: Niger Delta Field Structures and Associated Traps (Owoyemi, 2004).

Noteworthy, hanging-wall rollover anticlines were formed because of listric-fault geometry and differential loading of deltaic sediments above ductile shales. More enigmatic structures, cut by swarms of faults with varying amounts of throw, include collapsed-crest features with domal shape and strongly opposing fault dips at great depth (see Figure 2.1 from Owoyemi, 2004).

2.1.1 Review of the Stratigraphy.

Stratigraphic evolution of the Tertiary Niger Delta and underlying Cretaceous strata is described by Short and Stauble (1967). Allen (1965) described depositional environments, sedimentation

and physiography of the modern Niger Delta. Evamy *et al.* (1978) described the hydrocarbon habitat of tertiary Niger Delta.

The three major lithostratigraphic units defined in the subsurface of the Niger Delta which reflect the overall regression of depositional environments within the Niger Delta clastic wedge are, the Benin, Agbada and Akata formations (increase in age basin ward) (See Figure 2.2).

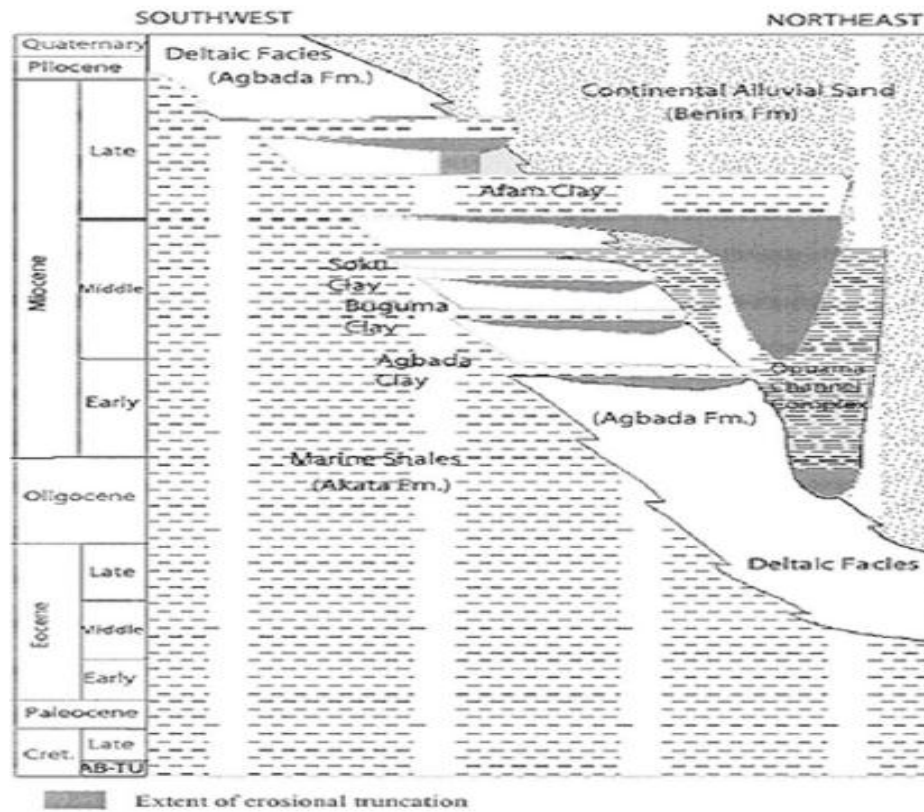


Figure 2.2: Stratigraphic Column Showing Formations of the Niger Delta (Owoyemi, 2004).

Stratigraphic equivalent units to these three formations are exposed in southern Nigeria (Table 2.1). The formations show a coarsening-upward progradational clastic wedge (Short and Stauble, 1967), deposited in marine, deltaic, and fluvial environments (Weber and Daukoru, 1975; Weber, 1986).

The Benin Formation comprises of the top part of the Niger Delta clastic wedge, from the Benin-Onitsha area in the north to beyond the present coastline (Short and Stauble, 1967). Its type section is Elele 1 Well, drilled about 38 km North-Northwest of Port Harcourt (Short and Stauble, 1967). The top of the formation is the recent subaerially-exposed delta top surface and its base extends to a depth of 4600 feet which is defined by the youngest marine shale. Shallow parts of the formation are composed entirely of non-marine sand deposited in alluvial or upper coastal plain environment during progradation of the delta (Doust and Omatsola , 1989). The age of the formation is estimated to range from Oligocene to Recent (Short and Stauble, 1967), it thins basin ward and ends near the shelf edge.

The Agbada Formation is defined in the Agbada 2 Well, drilled about 11 km North-Northwest of Port Harcourt (Short and Stauble, 1967). The well reached a total depth of 9500 feet without penetrating the base of the formation (the base was defined as the top of the Akata Formation in Akata 1 well). The formation usually called the Ogwashi-Asaba formation, occurs throughout Niger Delta clastic wedge, having a maximum thickness of about 13,000 feet and crops out in Southern Nigeria (between Ogwashi and Asaba) (Doust and Omatsola, 1989). The lithologies consist of alternating sands, silts and shales arranged within ten to hundred feet successions defined by progressive upward changes in grain size and bed thickness. The strata are generally interpreted to have formed in fluvial-deltaic environments and ranges in age from Eocene to Pleistocene.

The type section of the Akata Formation was defined in Akata 1 Well, 80 km east of Port Harcourt (Short and Stauble, 1967). A total depth of 11,121 feet (3, 680 m) was reached in the

Akata 1 well without encountering the base of this formation. The top of the formation is defined by the deepest occurrence of deltaic sandstone beds (7,180 feet in Akata well). The lithologies are dark gray shales and silts, with rare streaks of sand of probable turbidite flow origin (Doust and Omatsola, 1989). Marine planktonic foraminifera make up to 50% of the microfauna assemblage and suggest shallow marine shelf deposition (Doust and Omatsola, 1989).

Table 2.1: Formations of the Niger Delta Area (Modified from Short and Stauble, 1967).

SUBSURFACE			SURFACE OUTCROPS		
YOUNGEST KNOWN AGE		OLDEST KNOWN AGE	YOUNGEST KNOWN AGE		OLDEST KNOWN AGE
Recent	Benin Formation	Oligocene	Pleistocene	Benin Formation	
Recent	Agbada Formation	Eocene	Miocene Eocene	Ogwashi Asaba Formation Ameki Formation	Oligocene Eocene
Recent	Akata Formation	Eocene	Lower Eocene	Imo Shale Formation	Paleocene

Ages of the formation ranges from Paleocene to Recent (Doust and Omatsola, 1989). Those shales, formed during the early development stages of Niger Delta progradation, are thickest along the axis of the Benue and Bida Troughs. Akata shales were interpreted to be deepwater low

stand deposits by Stacher (1995). The formation grades vertically into the Agbada Formation with abundant plant remains and micas in the transition zone (Doust and Omatsola, 1989).

2.1.2 Review of the Hydrocarbon Occurrence.

Most of the hydrocarbon accumulations in the Niger delta have been found in the sandstones of the Agbada formation and are mainly trapped in roll-over anticlines fronting growth faults. The extent of the accumulation may or may not be restricted by subsidiary growth faults or antithetic faults cutting the anticline. This restriction becomes more evident on the larger anticlines, which, because of the size and extent of their crestal area, tend to form a less efficient focus for migration (Short and Stauble, 1967).

According to Short and Stauble (1967), in addition to these anticlinal traps, hydrocarbons have also been found in fault traps that are not closed on all sides by dip. Fields, particularly those in the roll-over anticlines, are normally of the multi-reservoir type. However, few, if any, of the reservoirs found are full to the structural spill-point and many contain no hydrocarbons at all.

The reservoirs of the Agbada formation according to short and Stauble (1967) are typically channel and barrier sandstone bodies similar to those of the recent delta with high porosity and permeability values (up to 40% and 1- 2 darcys, respectively). Oil found in the Agbada formation is of the paraffinic type with very low sulfur and asphaltene contents. The wax content ranges from less than 1% to 10%, and up to 20% in some reservoirs, whereas pour points may range from below -35°C to more than +30°C and specific gravities ranging from 15° to 50°API. Great variations in one or more of these characteristics have been observed within a single multi-

reservoir field. Little or no evidence of a well-developed pattern of distribution of oil types has emerged from discoveries made so far, beyond the conventional tendency toward lighter oil and more gas at greater depths. This large variation in the hydrocarbon content of Niger delta fields, and the discontinuous nature of the sandstone reservoirs evidenced by the difficulties of inter-field correlation, proves that there was no distant migration of oil. As the oil migrates only a relatively short distance updip into the nearest trap available at the time the oil migrated. Therefore, the most obvious source rocks are the shales of the Agbada formation itself and of the upper part of the Akata formation, which lies close to the sandstone reservoirs. Such a simple picture would explain most easily the distribution of hydrocarbons through the Niger Delta sediments so far as they are known today (Short and Stauble, 1967).

The Source rocks in the Niger Delta include marine interbedded shale in the Agbada formation, marine Akata formation shales and underlying Cretaceous shales (Evamy *et al.*, 1978; Ekweozor and Okoye, 1980; Lambert-Aikhionbare and Ibe, 1984; Bustin, 1988 and Doust and Omatsola, 1990). Reservoir intervals in the Agbada Formation have been interpreted to be deposits of high stand and transgressive system tracts in proximal shallow ramp settings (Evamy *et al.*, 1978). The reservoirs range in thickness from less than 45 feet to a few with thicknesses greater than 150 feet (Evamy *et al.*, 1978). Consequently, reservoirs may thicken towards down-thrown sides of growth faults (Weber and Daukoru, 1975). Structural traps formed during synsedimentary deformation of the Agbada formation (Evamy *et al.*, 1978), and stratigraphic traps formed preferentially along the delta flanks define the most common reservoir locations within the Niger Delta complex. The primary seal rocks are interbedded shales within the Agbada formation. Three types of seal are recognized:

- i. Clay smears along faults.
 - ii. Interbedded sealing units juxtaposed against reservoir sands due to faulting.
 - iii. Vertical seals produced by laterally continuous shale-rich strata (Doust and Omatsola, 1990).
- Major erosion events of early to middle Miocene age formed canyons which filled with shale; these fills provide top seals on the flanks of the delta for some important offshore fields (Doust and Omatsola, 1990).

2.2 Overview of the Meren Field

An overview of the Meren field is presented to help the reader understand some of the characteristics of the Offshore Niger Delta (OND) field, which is loosely patterned after the Meren field. The Meren field which is located offshore Nigeria contains 1.3 billion barrels of original oil in place (OOIP) and may be classed as a major oil accumulation. The more landward-lying fault blocks within the field contain an increasing greater preponderance of oil to gas reserves. The reservoirs are composed of sandstone with minor accumulations of authigenic kaolinite (Poston *et al.*, 1981). According to Poston *et al.* (1983), the Meren field is jointly owned by Nigerian National Petroleum Corporation (NNPC) 60% and Gulf Oil Company (now Chevron) 40%. However, the field is operated by Gulf Oil Company, Nigeria Limited (now Chevron Nigeria Limited).

The field is located offshore Bendel State (now Delta State), approximately 25 miles north-west of the Chevron/NNPC Escravos River Tank Farm and Export Terminal (Figure 2.3). The water depth in the field varies from 48ft to 60ft (Poston *et al.*, 1981).

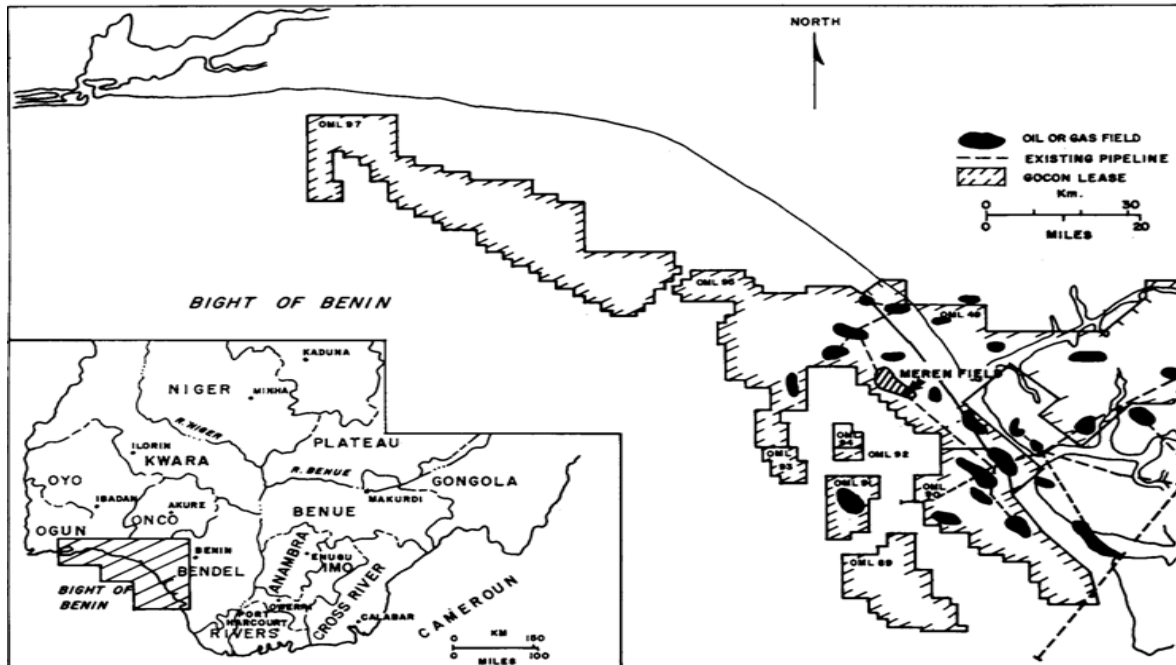


Figure 2.3: Location of Meren Field Offshore Nigeria (Source: Poston *et al.*, 1981)

Poston *et al.* (1981) stated that fifty-seven wells had been drilled in the Meren field, three of which are dry holes. The field was discovered in 1965, and production began in September 1968, by July 1, 1980, the field had produced 347,194, 961 STB Oil, 321, 545, 190 Mcf gas, and 10,123,132 bbl water with cumulative recovery of 26% OOIP. According to performance analysis (Poston *et al.*, 1981), the field appears to be producing by depletion-drive/gas cap expansion mechanism and majority of the reservoirs in this field are being affected by minimal water influx. Consequently, accumulation of oil and gas within the field is predicted according to the position of a particular fault block within the megastructure. The more downthrown fault block is gas prone and majority of the reservoir sands in the field exhibit in-situ porosities of 27% to 32%, with the sand permeabilities varying from 500md to 2,000md. The sands are well sorted with porosity and permeability values of a sand sample being affected principally by the clay type, clay origin and clay-size/pore throat size ratio. The horizontal/vertical permeability

ratio exceeds 10 only for permeabilities of less than 30md to 40md in the microscopic sense (Poston *et al.*, 1981).

Lumley *et al.* (2000) conducted a 4D seismic project at the Meren field, with an overview of the field specifics, seismic acquisition and processing details with 4D interpretation. A detailed quantitative 4D seismic analysis of the E-05 sands was also carried out by Lumley *et al.* (2000) which suggest that the seismic image of heterogeneous fluid flow is much more complex than that suggested by well data alone.

Importantly, Lumley *et al.* (2000) noted that there are six major fault blocks, each block containing up to a dozen productive reservoir sands, with more than 40 total producing sands. The total estimated original oil in place is 1.8 billion barrels, of which about 750 million barrels have been produced to date. Recovery factors are typically high in reservoirs with good pressure maintenance through water injection or aquifer support and over 80 producers and injector wells have been drilled to date. More so, current production from the field is about 85,000 barrels of oil per day, with a productive sands range in depth from 4,800 to 9,500 feet. The reservoirs are part of a set of sand-shale retrograde/prograde near-shore depositional sequences.

Many of the reservoirs, as stated by Lumley *et al.* (2000) but not all are below bubble point and have gas caps that have enlarged or decreased during production, which can complicate 4D seismic monitoring of oil and water. The oil is fairly live seismically at Meren with an average solution GOR of 400 scf/stb, giving a good compressibility contrast with reservoir brine that is advantageous for seismic monitoring of oil-water saturation fronts.

2.2.1 Geology and Reservoir Characteristics

The geologic description of the Meren field fits into the general deltaic sequence of the Niger Delta as described by Poston *et al.* (1981). A paleogeographic reconstruction of the depositional history shows that the major field pays were deposited in close proximity to a fluvial channel mouth. These sediments were transported by tidal and along-shore currents and re-deposited in a lower-energy regime of a tidal flat to a lower-barrier-bar environment.

The sands are moderately well sorted, fine to very fine grain sudarkosic sandstones and the shales are soft claystones that grade from medium to hard with increasing depth. The Agbada formation is the oldest stratigraphic unit encountered on the Meren field and is of Middle Miocene age. X-ray diffraction and scanning electron microscope (SEM) analysis indicate that the dominant clay mineral is authigenic kaolonite (Poston *et al.*, 1983). These clay particles generally occur in the pores and pore throats as booklets and platelets ranging in size from 43 to less than 2 microns as can be seen in figure 2.4 below.

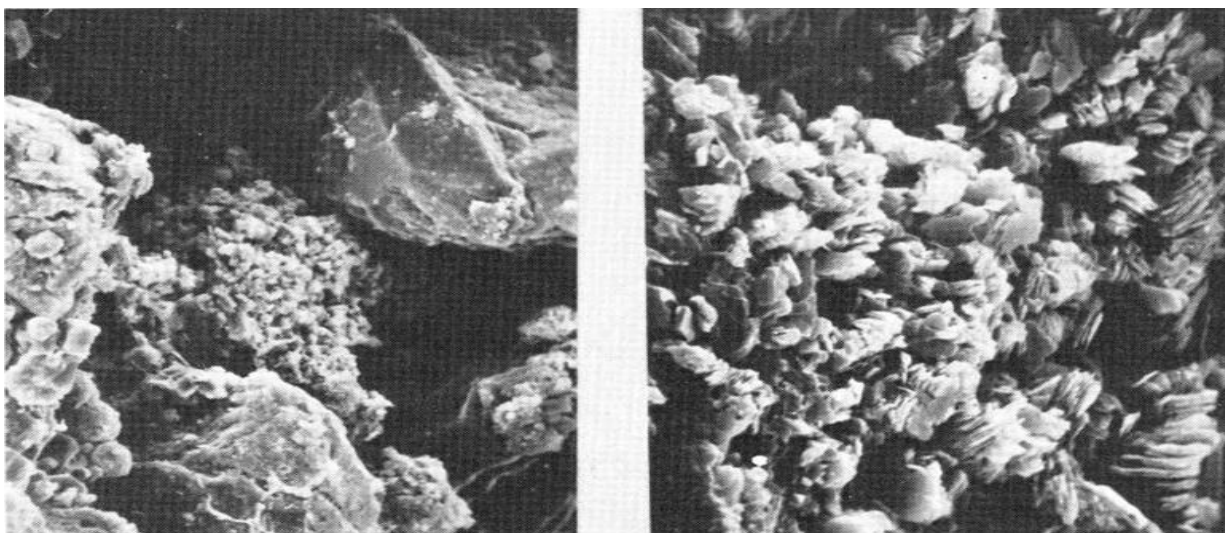


Figure 2.4: Scanning Electron Microscope (SEM) Photos (Source: Poston *et al.*;1981).

Furthermore, Poston *et al.* (1983) presented that the Meren field is typified by structure Map G-01 as can be seen in figure 2.5. Fault blocks A and B comprise of the major oil productive areas occurring within a rollover anticlinal structure bounded on the North-East and on the South-West by two major growth faults, designated I-I' and II-II' in figure 2.6 and both possessing displacements of at least 1,500ft (Poston *et al.*, 1981). The Southern-lying fault (II-II') divides the field structure into two dissimilar producing regions. While, the northern fault blocks A and B is predominantly oil productive, the southern fault block "F" is mainly gas bearing. Subsidiary oil production also has been found in the smaller C, D and E producing segments (Poston *et al.*, 1981).

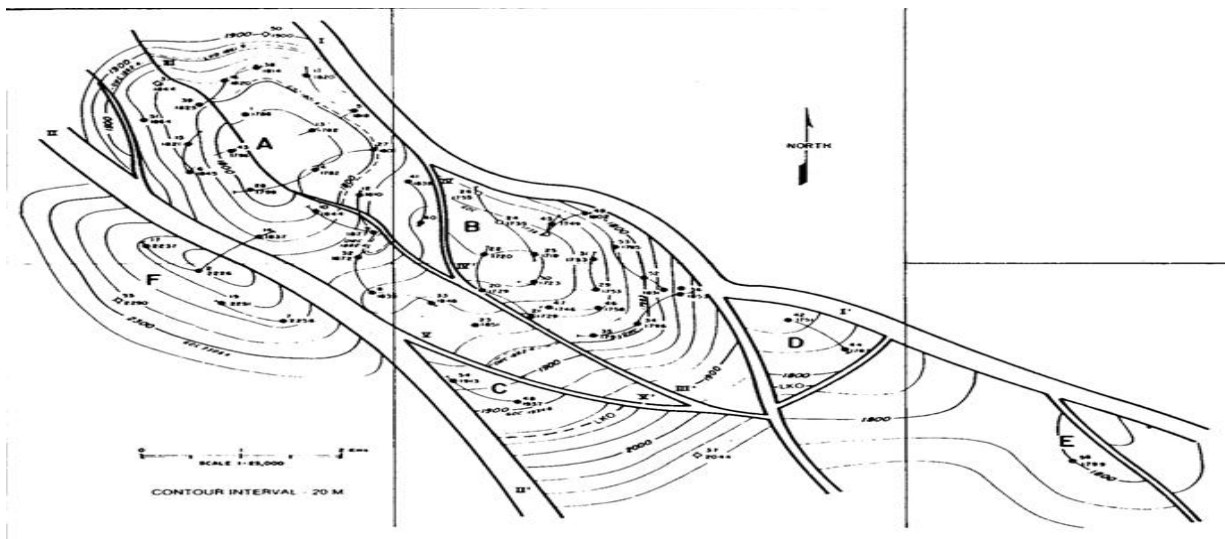


Figure 2.5: Sand G1 Structure Map (Source: Poston *et al.* 1981).

More so, subsidiary oil production has been found in the smaller C, D and E producing segments which were caused by minor relief faults forming small traps against the major growth faults. These fault blocks are peripheral to the Meren field proper and do not figure significantly in the discussion of the field characteristics (Poston *et al.*, 1981).

2.2.2 Occurrence of Hydrocarbon

The reservoir sands of the field have been paleontologically dated as between Lower Pliocene and middle Miocene age. Individual sands vary in thickness from 121ft to 16ft, typically of a centrally located well within a given fault block. However, the thickness of given sand may increase dramatically in positions close to growth fault (Poston *et al.*, 1981).

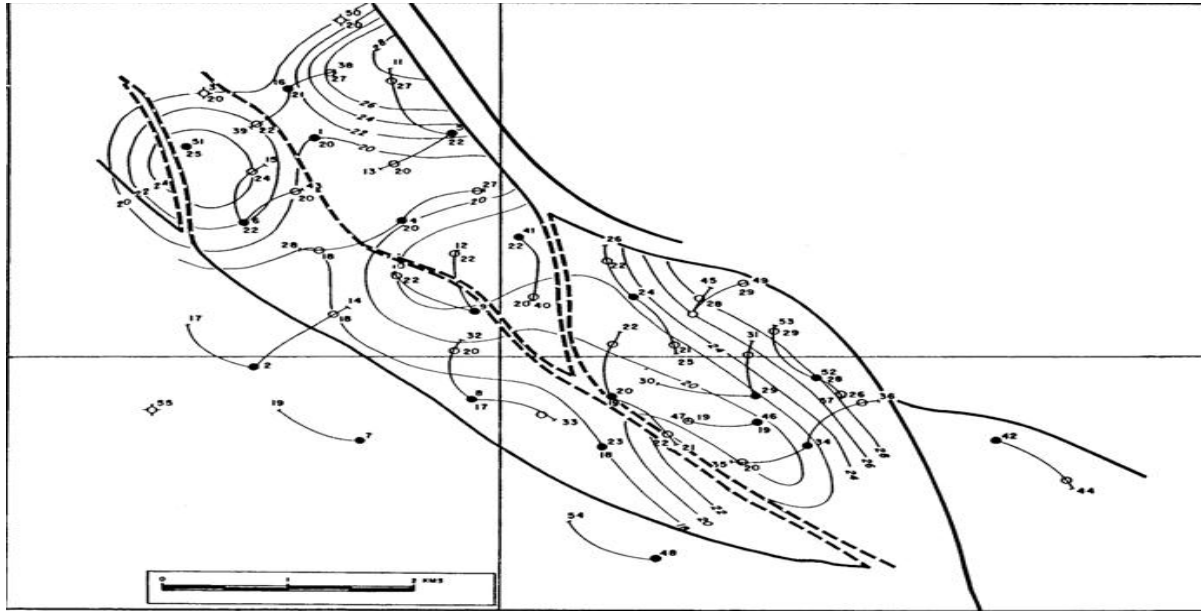


Figure 2.6: Sand G1 Isoporosity Map (Source: Poston *et al.*, 1981).

From figure 2.7 below, the fault Block B contains the greatest number of oil producing intervals with average porosity values ranging from 23% to 31% and permeability values ranging from 75md to 3,000md. However, most of the productive intervals usually exhibit permeability values from 500 to 1,000md.

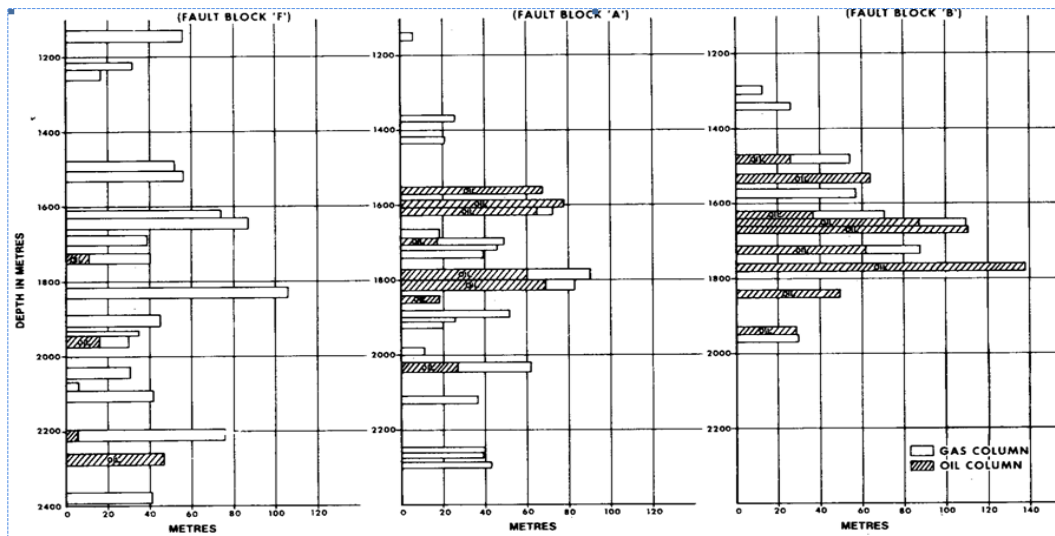


Figure 2.7: Hydrocarbon Content in Fault Blocks A, B, and F (Source: Poston *et al.*, 1981).

According to Poston *et al.*, (1981), oil production from the Meren field comes mainly from fault blocks A and B. The hydrocarbon distributions within the three major areas of the Meren field are compared in figure 2.7. The figure relates the relative thickness of the oil and gas column present in fault blocks A, B, and F. The striking difference in the hydrocarbon content of the fault block is shown by the bar graphs. Also, there is the preponderance of gas in the Southern lying fault block F and volumetric estimates indicate that 93% of the hydrocarbon pore space is occupied by gas (Poston *et al.*, 1981).

The sand units of fault blocks A and B are correlative and the hydrocarbon distribution between the relative oil and gas volumes are comparable for both fault blocks. Nevertheless, the oil columns in fault block B are the longest found in the Meren field with columns varying in height from 85ft to 453ft. Volumetric calculations indicate that 86% of the hydrocarbon-bearing pore space contains oil, while the remaining 14% contains gas (Poston *et al.*, 1981). According to Poston *et al.* (1981), there are three major reservoirs of interest in fault block A. Those elongated,

North-West/South-East-trending reservoirs are designated reservoirs E1/A, G1-G2/A, and H4/A. The most East-lying, fault block B, is a domal feature that contains five reservoir candidates namely E1/B, E5/B, G1/B, G2/B, and H1/B. The reservoirs and average rock properties are listed in table 2.2 below.

Table 2.2: Reservoir Properties and Production Summary (Modified from Poston et al, 1981).

RESERVOIR PROPERTIES					CUMULATIVE PRODUCTION (JUNE 1980).			
Reservoir	Φ (%)	S_{wi} (%)	K (md)	R_{si} (cu ft/bbl)	OOIP (MM STB)	Oil (MM bbl)	Gas (Bcf)	Water (MM bbl)
E1/B	28	18	1.0	333	40.8	8.1	2.3	1.4
E1/A	26-31	15-24	1.0-1.5	434	172.0	45.8	28.4	0.6
E5/B	27-30	15-22	0.3-1.0	476	218.1	44.2	24.2	1.8
G1/B	25	21	0.2-0.6	516	65.6	19.2	13.5	0.1
G2/B	32	14	1.8	566	276.8	58.8	32.1	0.0
G1-G2/A	27	24	1.2	602	281.5	83.8	55.6	1.2
H1/B	27	20	0.3-0.5	566	65.1	20.7	14.1	0.9
H4/A	23-28	25-30	0.1-0.5	801	50.4	13.9	18.0	0.1
TOTAL					1,170.3	294.5	188.2	6.1

Evamy *et al.* (1978), compiled data from fields located in the Niger delta. They concluded that 71% of the oil bearing reservoirs had oil columns heights of 50ft or less, while, only 5% of the reservoirs had oil columns heights of 148ft or greater. Poston *et al.* (1983) compared these statistics of the Meren field with those of Evamy *et al.* (1978) and it was apparent that the oil accumulation characteristics of fault block B did not fit the norm. Importantly, Poston *et al.* (1981) pointed that the ability of these reservoirs to be filled beyond the intersection of the major growth fault is critical for the formation of the unusual large oil accumulations. In addition, it was indicated that the oil columns in the five oil-producing sands in fault block B extend below the point of intersection with the fault plane of the major growth fault.

2.2.3 Rock Properties

Routine core analyses have been performed on core samples from the field and surface conditions showed a porosity range of 18% to 36% as stipulated by Poston *et al.* (1981), with permeabilities ranging from 10md to 9,600md. Furthermore, as presented by Poston *et al.* (1981), the permeability of the Meren field sands was found to be a function of the clay content. This can be seen in figure 2.8 which shows the relation of the clay content in the sample to some measured porosity. The small data spread indicates that the sands possess the same basic character.

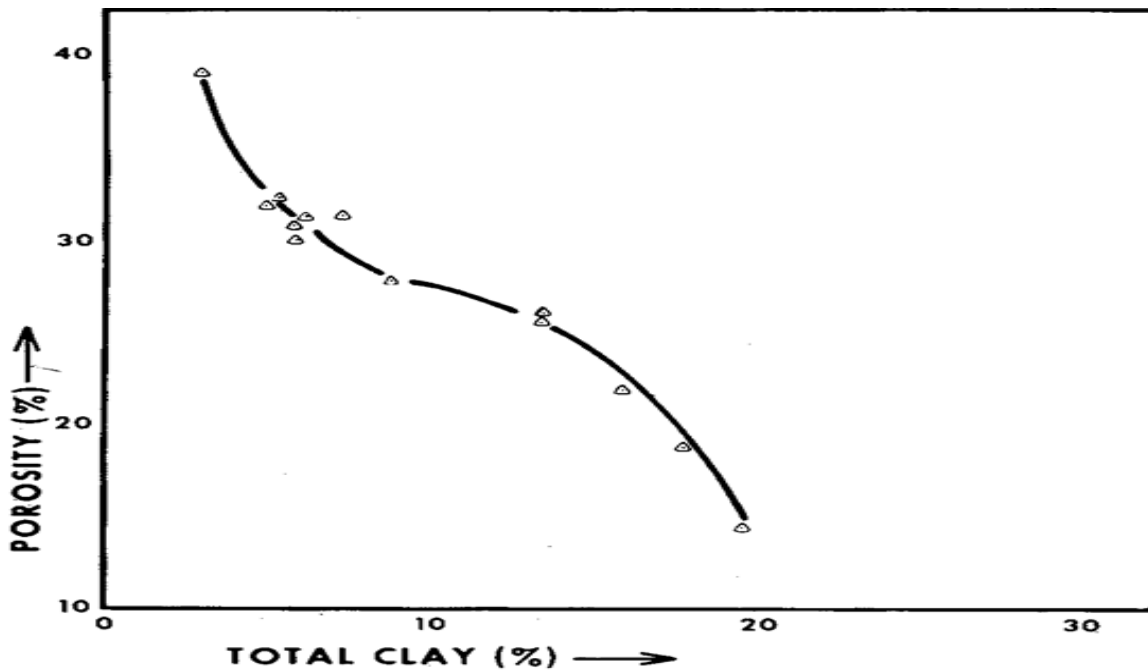


Figure 2.8: Relation of Porosity to Clay Content (Source: Poston *et al.*; 1981).

2.2.4. Rock Sensitivity

From the analysis of the producing behaviour according to Poston *et al.* (1981), the Meren field showed that some type of enhanced recovery project eventually must be installed to improve the ultimate recovery. Water filtration tests conducted during 1978 and 1979 proved that seawater

could be easily treated and used. Water sensitivity analyses has also been conducted on a number of core samples from the field and were found to be relatively insensitive to both sea water and diluted water. Furthermore, it has been discovered that the cleanest and greatest sections in the sand G-01 occur closest to the downthrown side of the growth faults, which is also the lowest structural position in the reservoir (Poston *et al.*, 1981).

2.3 Overview of Uncertainty Evaluation

What do we mean by uncertainty? It means being less than 100% sure about something. In the petroleum industry, people are extremely concerned about quantities such as original hydrocarbon in place, reserves, and the time for the recovery process, which are all critical to the economic returns. Those quantities play a key role in making important decisions for both the oil producers and the investors at different phases of reservoir development. However, being certain of these quantities is usually impossible (Zhang, 2003).

In the past 10 to 15 years, probabilistic expressions of reserve estimates have been gradually accepted and adopted in the industry (Zhang, 2003). The traditional method involves specifying a deterministic value for the reserve's estimate, which usually is calculated with a mathematical model. Unlike the probabilistic method, the traditional method does not consider the uncertainty associated with the reserve estimate; it simply takes for granted that the deterministic reserve value is the most likely value. As a matter of fact, when we talk about reserves prediction, we are never completely sure about its correctness: there is always some degree of uncertainty, big or small, associated with it. Therefore, a statistical approach or probabilistic approach is more appropriate for STOOIP prediction.

As noted by Zhang (2003), uncertainty comes from several sources: measurement error, mathematical model error, and incomplete data sets. All field and laboratory measurements, such as production and PVT data, involve some degree of error or inaccuracy, which may result from poor tool calibration or even human error. This kind of error can be reduced to some extent by using more accurate tools or increased human effort, but can never be eliminated. When geoscientists and engineers try to evaluate the values of reservoir parameters from various mathematical models, uncertainty is incurred. None of the mathematical models are perfect because they were built either by empirical methods or on the basis of assumptions that are not always applicable to the real situations. The development of a finite-difference reservoir simulator involves some assumptions and numerical computational error. In real situations, complete data set are never obtained for the study. Often, there is lack of some data and thus reasonable guesses are made based on the knowledge and experience and the process of course, introduces errors to the prediction.

The paucity of available data in the appraisal stage of a field, or incomplete reservoir description even during the development stage, increases the risks associated with investment decisions. As presented by Slamao and Grell, (2001), quantification of these uncertainties and evaluation of the risks would improve decision making. However, estimating these uncertainties is complicated because it requires an understanding of both the reservoir's static structure and dynamic behaviour during production (Zhang, 2003). Notwithstanding, even a producing field can result in financial loss (Capen, 1975 and Garb, 1986) and also mature fields have uncertainties in the reservoir description.

Uncertainty analysis methods provide new and comprehensive ways to evaluate and compare the degree of risk and uncertainty associated with each investment choice. The result is that the decision-maker is given a clear and sharp insight into potential profitability and the likelihood of achieving various levels of profitability. In this present study, uncertainty analysis for the reserves prediction, refers only to technological uncertainty. Here, the reserve's distribution is not converted into monetary value distribution, which is usually done in risk analysis. However, the reserves distribution can be converted into net present value distribution once an oil and gas price prediction is made (Zhang, 2003).

Uncertainty evaluation methods attempt to reduce the complexity and difficulty of quantifying uncertainty. As stated by Garb (1986), uncertainty analysis methods have some advantages:

- Uncertainty analysis forces a more explicit look at the possible outcomes that could occur if the decision-maker accepts a given development scheme.
- Certain techniques of uncertainty analysis provide excellent ways to evaluate the sensitivity of various factors relating to overall worth.
- Uncertainty analysis provides a means to compare the relative desirability of various candidate projects.
- Uncertainty analysis is a convenient and unambiguous way to communicate judgments about risk and uncertainty.

Exceedingly complex investment options can be analyzed using uncertainty analysis techniques. As such, to economically develop reservoirs and maximize the return, oil producers have to characterize and, if possible, try to reduce the uncertainties (Zhang, 2003).

2.3.1 Uncertainty Evaluation in Oil in Place Volumes

According to Akinwunmi *et al.* (2004), at the discovery of a new field or extension of an existing field, there are uncertainties associated with quantifying the amount of hydrocarbons in place. These uncertainties may be related to the structure, aerial extent of the accumulation, unseen fluid contacts to delineate the vertical extent, internal architecture of the reservoir and the characteristics of the resident fluid(s).

In some cases, companies may complete and produce discovery wells before they can fully appraise the structure or may be forced by other considerations such as community disturbances to abandon appraisal drilling and continue to produce from existing well(s). All these and much more, have an impact on the evaluation of in-place hydrocarbon resources and consequently recoverable hydrocarbons. In Field Development Planning, it is a routine to identify and quantify the impact of major subsurface uncertainties such as the in-place volumes and their distribution (Akinwunmi *et al.*, 2004).

Akinwunmi *et al.* (2004) stated that lack of PVT samples and analyses also add to the uncertainty in fluid properties and the erratic distribution of petro-physical parameters also contributes to petro-physical uncertainties. More so, Akinwunmi *et al.* (2004) also estimated that the main uncertainties affecting the evaluation of OIIP for the G1.0 reservoir in the EGBM field are gross rock volume, porosity, hydrocarbon saturation – HC (Capillary pressure curves), net to gross ratio and formation volume factor.

2.3.2 Uncertainty Evaluation in Gas in Place Volumes

Aprilla *et al.* (2006) quantified uncertainty in original gas in place estimates with bayesian integration of volumetric and material balance analyses. Glimm *et al.* (2001) showed that the Bayesian approach can reduce the uncertainty in the prediction of unknown geological parameters in the simulation of an oil field. On the other hand, Galli *et al.* (2004) used the Bayesian approach to evaluate new information for choosing between different exploitation scenarios for a gas field. In 2004 Ogele *et al.* (2004) used the Bayesian approach to combine volumetric and material balance methods and quantify uncertainty of OHIP estimates in gas-cap driven oil reservoir. They quantified the uncertainty of two parameters, original oil in place and relative gas-cap size, estimated using the Havlena and Odeh form of the material balance equation.

2.3.3 Uncertainty Evaluation in Forecasting Rate and Production Efficiency

Current techniques for production-data integration into reservoir models can be broadly grouped into two categories: deterministic and Bayesian. The deterministic approach relies on imposing parameter-smoothness constraints using spatial derivatives to ensure large-scale changes consistent with the low resolution of the production data. The Bayesian approach is based on prior estimates of model statistics such as parameter covariance and data errors and attempts to generate posterior models consistent with the static and dynamic data. Both approaches have been successful for field scale applications, although the computational costs associated with the two methods can vary widely (Vega *et al.*, 2004). The deterministic and Bayesian approach according to Vega *et al.* (2004) differ fundamentally in the way in which probability is introduced into the calculation and in their treatment of observed data and prior information. In

addition, the Bayesian approach associates probability with the prior information, whereas the deterministic approach treats it as fixed. In fact, in the deterministic approach, probability enters into the calculations only through the data errors, which generally have a random component associated with them. Nonetheless, both approaches have been used very successfully under a wide variety of reservoir conditions (Vega *et al.*, 2004).

2.3.4 Impacts on Uncertainty in Static and Dynamic Modelling

To a greater degree than most other operational environments, deepwater reservoirs have a very high degree of uncertainty and associated risks because of scarcity of reservoir data and the high costs of development. The wide ranges of reservoir data that could have significant impact on estimates of in-place hydrocarbon volumes, productivity, reservoir continuity, drive mechanism and reserves recovery require that the uncertainties associated with these data be examined in a systematic manner. In addition, the costs associated with well types, number of wells, completion costs and production systems are very uncertain (Ezekwe and Filler, 2005). Akinwumi *et al.* (2004) also used a multi-scenario static and dynamic modeling to quantify the impact of these uncertainties (gross rock volume, porosity, net to gross ratio, hydrocarbon saturation and formation volume factor) on both the static volumes and other parameters needed for a robust field development.

2.4 Overview of Various Methodologies of Accounting for Uncertainties

Akinwumi *et al.*, (2004) published a paper in 2004 that demonstrates the methodology and results of an integrated multi-disciplinary effort at translating uncertainties into a range of static (in-place) volumes for the purpose of field development. Erratic sand development, paucity of

biostratigraphic control coupled with a complex structure make the G1.0 complex of the EGBM field one of the least understood hydrocarbon reservoirs of the Northern depobelt – Onshore, Niger Delta.

An attempt has also been made by Akinwumi *et al.* (2004) in comparing results from the probabilistic volumetric evaluation of this reservoir and the deterministic (best estimate) method. They carried out the construction of 3-D static reservoir models based on the understanding of facies and their relationships, through the integration of all available data used to enhance the understanding and quantification of the uncertainties.

Uncertainty analysis carried out by Akinwunmi *et al.* (2004) on the EGBM field found that there were a lot of uncertainties in the structure of the G.1 sands, including petrophysical parameters (porosity, net-to-gross and hydrocarbon saturation) and the fluid parameters (due to the non-availability of fluid sample analysis).

2.4.1 Limitations and Shortcomings of Some Existing Uncertainty Methods

The Bayesian approach is particularly well suited for post-data inference, as it assigns probability to the model space. Bayes' theorem provides a mathematical basis for revising preliminary estimates of reservoir characteristics and their uncertainties when additional information becomes available. One major limitation is that large number of reservoir models might be needed before a good model that matches the production data is obtained.

According to Zhang (2003), the Monte Carlo method can be quite computationally intensive. In a situation where many independent variables are random and they all have large variabilities, a larger number of runs of the mathematical model may be needed to recognize the range of the dependent variable response. An important point about the Monte Carlo method is that the distribution of the output of the dependent variable is sensitive to the input parameter distributions.

To generate random numbers for the independent variables, probability density functions are needed for them. Thus, those probability density functions have to be determined before Monte Carlo method can be applied.

The Monte Carlo method is a statistical method; therefore, some knowledge of statistics is a prerequisite both for its correct application and for the interpretation of the results. This might be a barrier for its application in the industry. In addition, determining the input variable distributions and their character parameters involves some subjectivity.

Despite its limitations, Monte Carlo simulation has been widely used in the petroleum industry for risk analysis (Peterson *et al.*, 1995 and Komlosi,2001), project evaluation (Galli *et al.*, 1999 and Kokolis *et al.*, 1999) and even fracture-characteristic investigation (Han *et al.*, 2001).

CHAPTER THREE

3.0 METHODOLOGY

OND field is on the Western edge of the Niger River Delta about 110 miles South-East of Lagos. It lies about 8 miles offshore in approximately 40ft of water and production has mainly been from sand G. Fault block A of the G-1 actually acts as a single producing unit containing both sands G- 1 and G- 2. Similarly, the fault block referred to as B is believed to act as a single producing reservoir containing both sands G- 2 and G- 3. The work described here entails modeling the fault block A of the G-1 sands of the OND field.

The methodology used in this study is illustrated in figure 3.1 and the detailed procedure is described in the following section.

3.1 Geological Modeling

The basic inputs in the reservoir characterization process and for the geologic model were the geological skeleton, faults polygons for all major faults, petrophysical properties such as porosity, saturation, net-to gross thickness, area and Oil formation volume factor. Permeability was not included here because it actually has no effect on STOOIP. The structural map was digitized and gridded. Then, codes for each grid, area and zones were written and the grid file was imported into the Petrel platform.

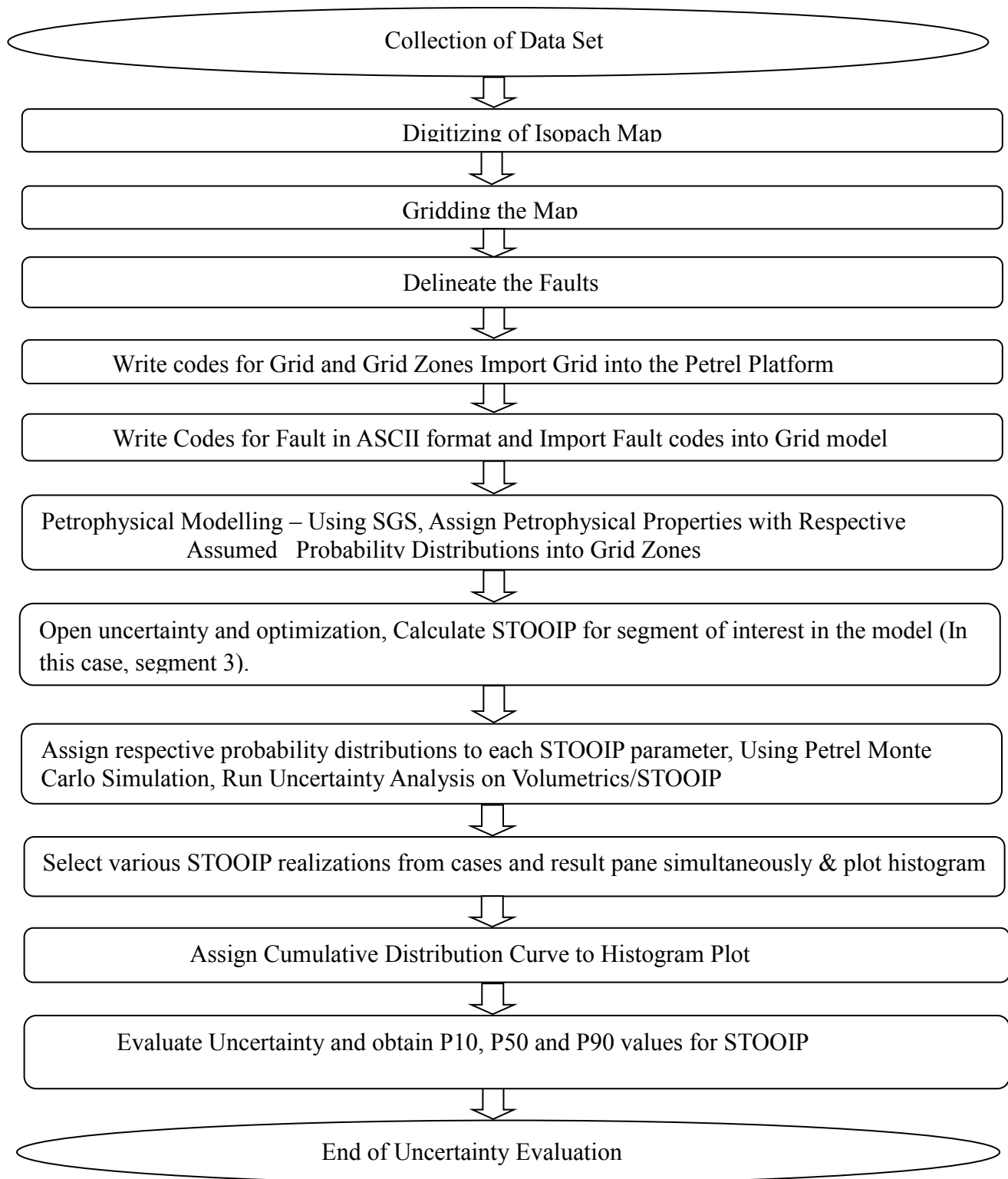


Figure 3.1 Workflow Used in the Grid-based Geologic Modeling and Uncertainty Evaluation.

In the following section we describe the Petrel workflow used in this study (Figure 3.1).

3.1.1. Horizon and Zone Modeling.

Five horizons were modeled for this reservoir to ensure the proper delineation of the oil section of the reservoir into zones. A total of four zones were created in this reservoir. The first three zones, counting from the top represented the hydrocarbon/oil zones. The fourth zone was considered as the water zone. This method of zonation of the reservoir is to account for reservoir heterogeneity in order to quantify the inherent uncertainties in the volumes of fluids in place (STOOIP) in the OND field.

3.1.2 Fault Modeling

The main geological feature in this field is a system of faults (shown in figure 3.2) that divides the field into eastern and western sections. The fault systems were modeled as vertical fault surfaces as shown in **figure 3.2**.

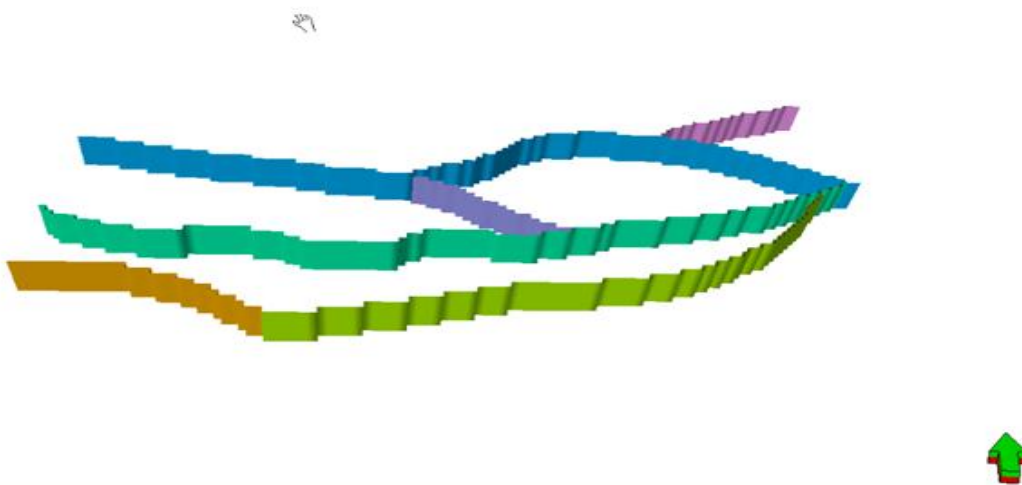


Figure 3.2: Grid Model Showing Fault Zones

The reservoir was also modeled with six faults, the various faults with their respective colours can be seen in Appendix 4D. The faults were modeled such that the major segment of interest was delineated (see Appendix D3b), thus dividing the model basically into five fault blocks termed segments (see Appendix D5). Uncertainty evaluation focused on the segment for fault block A (segment 3) because, fault block A is the most prolific segment of the G-1 sands in terms of oil originally in place and oil production.

3.2 Petrophysical Modeling

Various petrophysical properties (Porosity, Net-to-Gross, and Water saturation) were assigned and simulated with the model. The stochastic (SGS) method was used for modeling the distribution of continuous properties in the reservoir model.

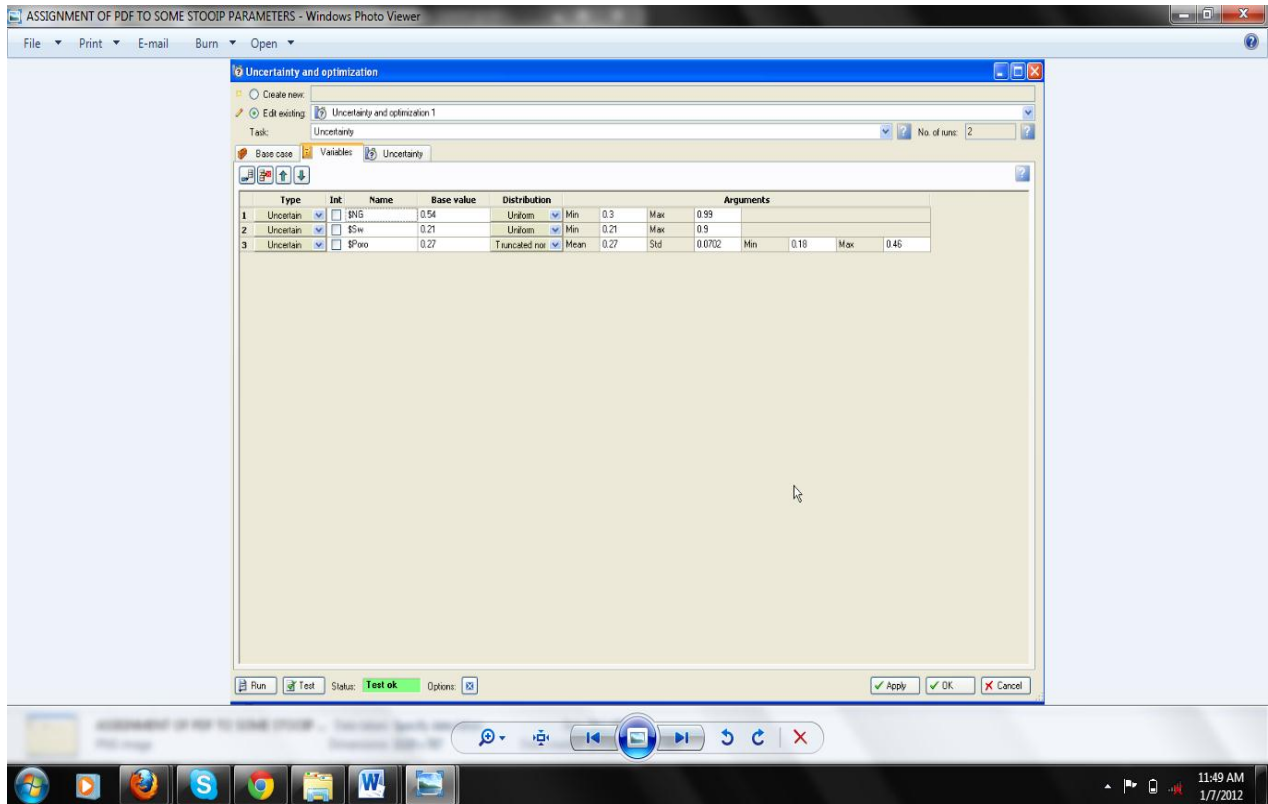


Figure 3.3 Assignment of Probability Distribution Functions to Petrophysical Properties

3.2.1 Porosity

Porosity was modeled in the G-1 Sand assuming a normal distribution. The mean, standard deviation, minimum and maximum values of porosity for the various realizations were created using the Petrel software. The sampling method used was the Monte-Carlo method (**figure 3.4**). The grid cells of the model were then populated with respective porosity values as can be seen in Figure 3.5.

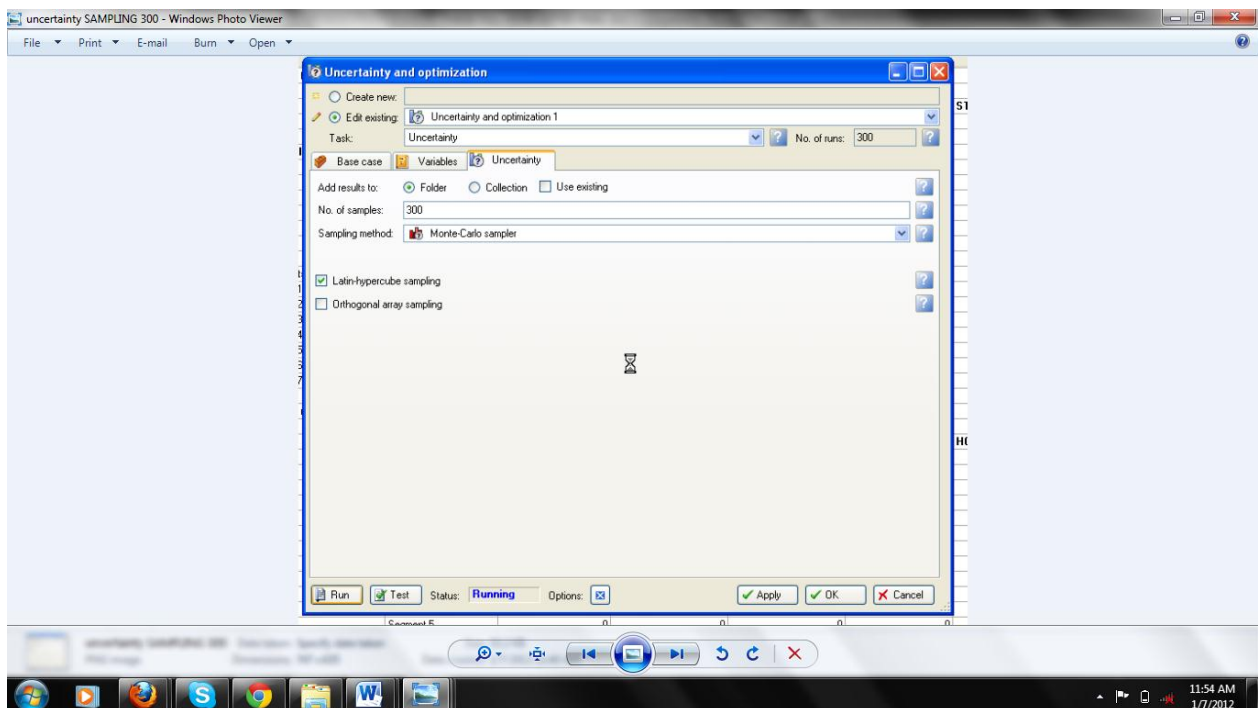


Figure 3.4 Uncertainty Sampling Method for Porosity

It is important to note here that zone 4 is actually the water leg and it was not included in the calculation of STOOIP.

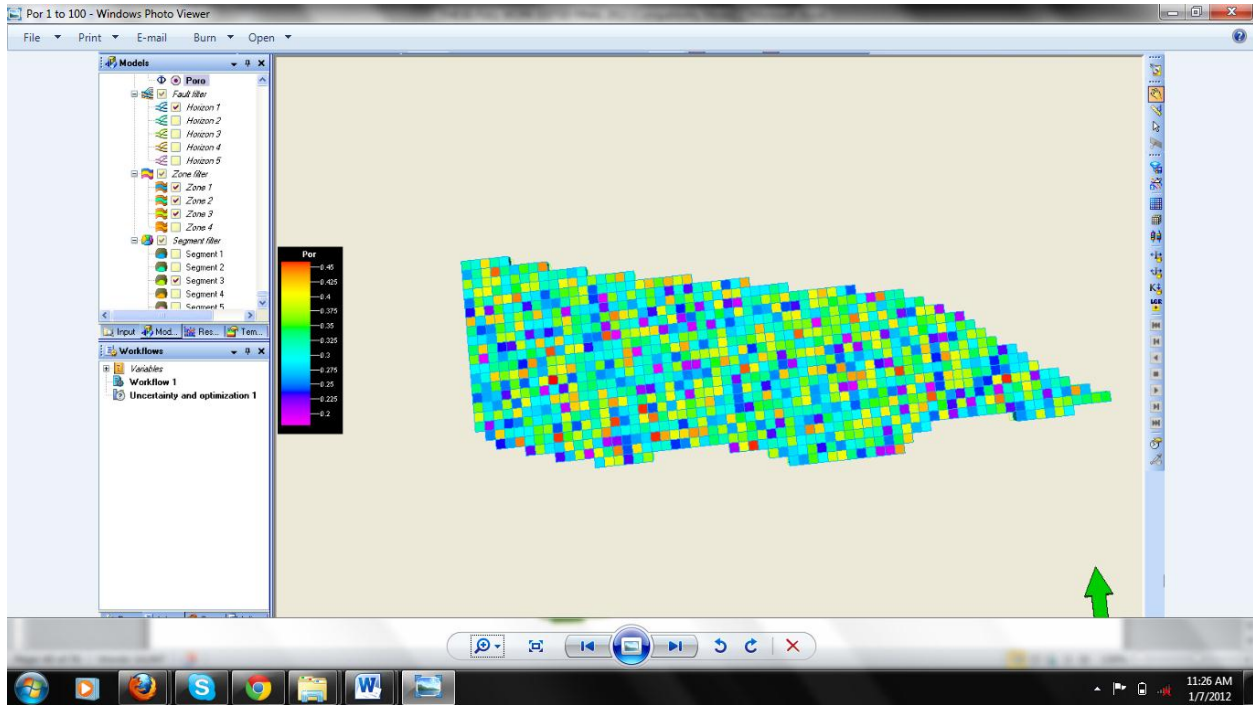


Figure 3.5: Example Realization of Porosity

3.2.2 Net-to-Gross Thickness Ratio

The net-to-gross thickness ratio was assumed to be uniformly distributed with a range between 0.3 and 1.0. Then 100 realizations of net-to-gross ratios were generated for each zone to calculate STOOSP. Figure 3.6 shows an example of the realizations of net-to-gross thickness derived in this study.

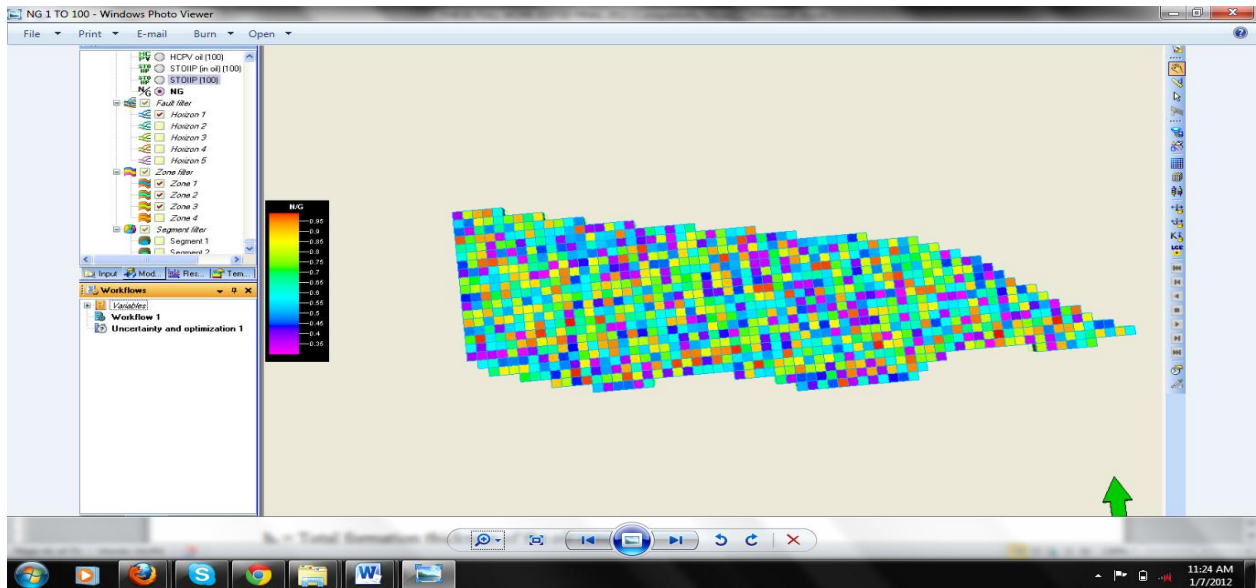


Figure 3.6: Example Realization of Net -to- Gross Thickness Ratio.

3.2.3 Water Saturation

Water saturation distribution at initial reservoir conditions was considered in this study. Water saturation (S_w) was assumed to be uniformly distributed with minimum and maximum values of 0.21 and 0.79 in the hydrocarbon zones. An example of S_w realization is shown in fig. 3.7.

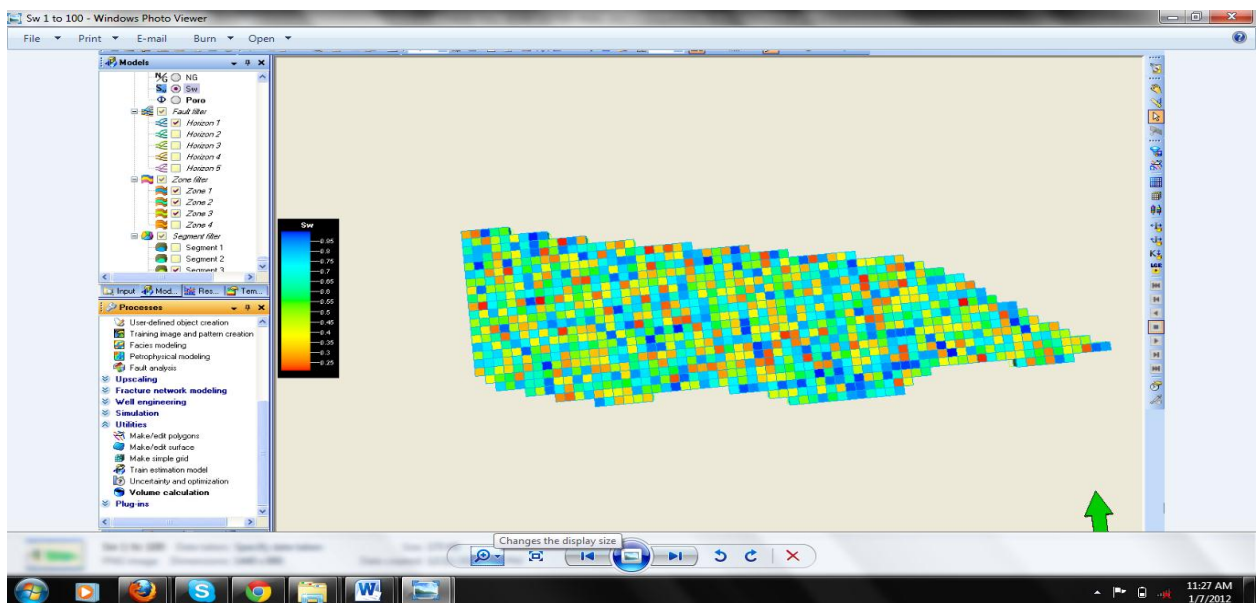


Figure 3.7: Example Realization of Water Saturation

3.3 Uncertainty Evaluation of Volumes of Fluids in Place (STOOIP)

The goal of this work is to evaluate uncertainty of the volume of fluids in place (STOOIP) in the G-1 Sands of the OND field. The STOOIP for each zone was determined from equation 3.1.

$$\text{STOOIP} = \frac{7758 * A_r * h_t * (N/G) * \Phi * (1 - S_{wi})}{B_{oi}} \dots\dots\dots (3.1)$$

Where

B_{oi} = Oil Formation Volume Factor

A_r = Area of reservoir.

N = Net formation thickness

G = Gross formation thickness

h_t = Total formation thickness of the oil zone.

Φ = Porosity of the oil zones.

S_{wi} = Initial water saturation.

The area, gross thickness and oil formation volume factor were kept constant in this work. Using Equation 3.1 one hundred realizations of STOOIP were generated for each zone. The uncertainty in STOOIP was then evaluated using histogram plots to calculate the P10, P50 and P90 values.

A method and procedure for modeling the G-1 Sands of fault block A in the OND field has been presented. The method accounts for the uncertainty in the calculation for STOOIP in an oil reservoir.

CHAPTER FOUR

4.0 DISCUSSION OF RESULTS

The results of the volume of STOOIP calculated for Zones 1, 2, and 3 are shown in **Figures 4.1 to 4.3**. Monte-Carlo Direct Simulation (MCS) was utilized in the case study and hundred realizations of STOOIP were generated for each of the three zones.

A spreadsheet (Appendix E) was produced to show the raw input data and the probability distribution functions (PDF's) assigned to each STOOIP parameter. Uncertain parameters which include: porosity, net-to-gross and water saturation were analyzed and STOOIP values for each simulation case were plotted as histograms. Then, P10, P50 and P90 values (**see table 4.1**) were analyzed in order to evaluate the uncertainty in STOOIP. The results of the uncertainty analysis of STOOIP in the G-1 Sands are visualized as histograms with cumulative distribution functions (**see figures 4.1, 4.2 and 4.3**).

A cumulative distribution function (CDF) which gives a probability (e.g., probability of $S(x) < s$ for all s) was displayed based on the histogram intervals and the curve drawn from the mid-point. The P10, P50 and P90 levels are shown in the histogram plot when the distribution function was displayed. Table 4.1 lists the STOOIP for the three hydrocarbon zones of the Fault Block A of the G-1 Sands studied in this work. The results are discussed for each Zone.

4.1 STOOIP for Zone 1

Recall Zone 1 is the topmost zone in the G-1 Sands model. The results shown in Table 4.1 indicate that the P10 value for STOOIP is 17.9MMSTB, P50 value is 45 MMSTB and the P90 value for STOOIP is 104.7MMSTB. The P10 shows a 10% probability of getting a volume of fluids in place lesser than 17.9MMSTB. This is equivalent to a 90% probability of getting a STOOIP greater than 17.9MMSTB. Fig. 4.1 shows the histogram of STOOIP for Zone 1 of the G-1 Sands in the OND field.

Table 4.1: STOOIP of Fault Block A of the G-1 Sands in MMSTB

Percentiles	STOOIP (MMSTB)		
	P10	P50	P90
Zone 1	17.9	45.0	104.7
Zone 2	14.9	37.5	87.2
Zone 3	11.9	30.0	69.8

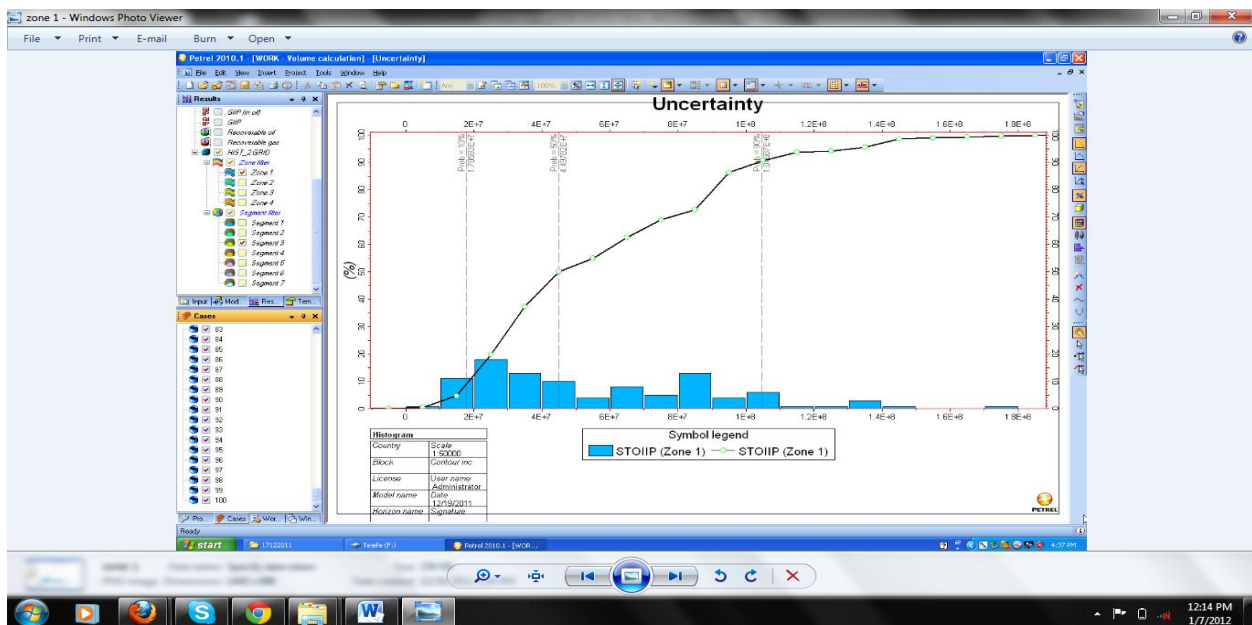


Figure 4.1: Histogram Plot of STOOIP for Zone 1

4.2 STOOIP Results for Zone 2

As shown in figure 4.2 that the STOOIP for Zone 2 ranges from a minimum of 14.99MMSTB for P10 to a maximum of 87.2MMSTB for P90. These results show that Zone 1 of the Fault Block A contains more oil in place than Zone 2 of the G-1 Sands of the OND field.

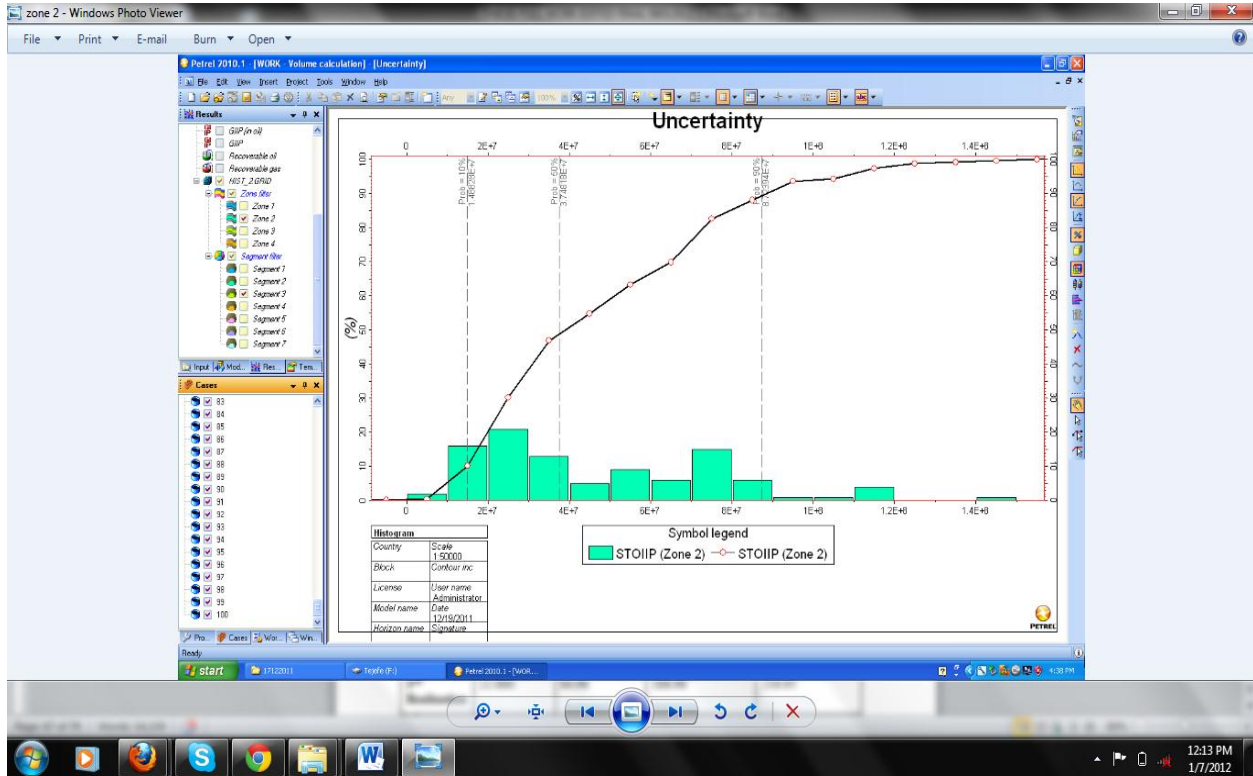


Figure 4.2: Histogram Plot of STOOIP for Zone 2

4.3 STOOIP for Zone 3

Figure 4.3 shows the results of STOOIP in Zone 3 of the G-1 Sand. The data show that the P10 STOOIP for this zone is 11.9MMSTB; the P50 is 29.8MMSTB, and the P90 is 69.8MMSTB.

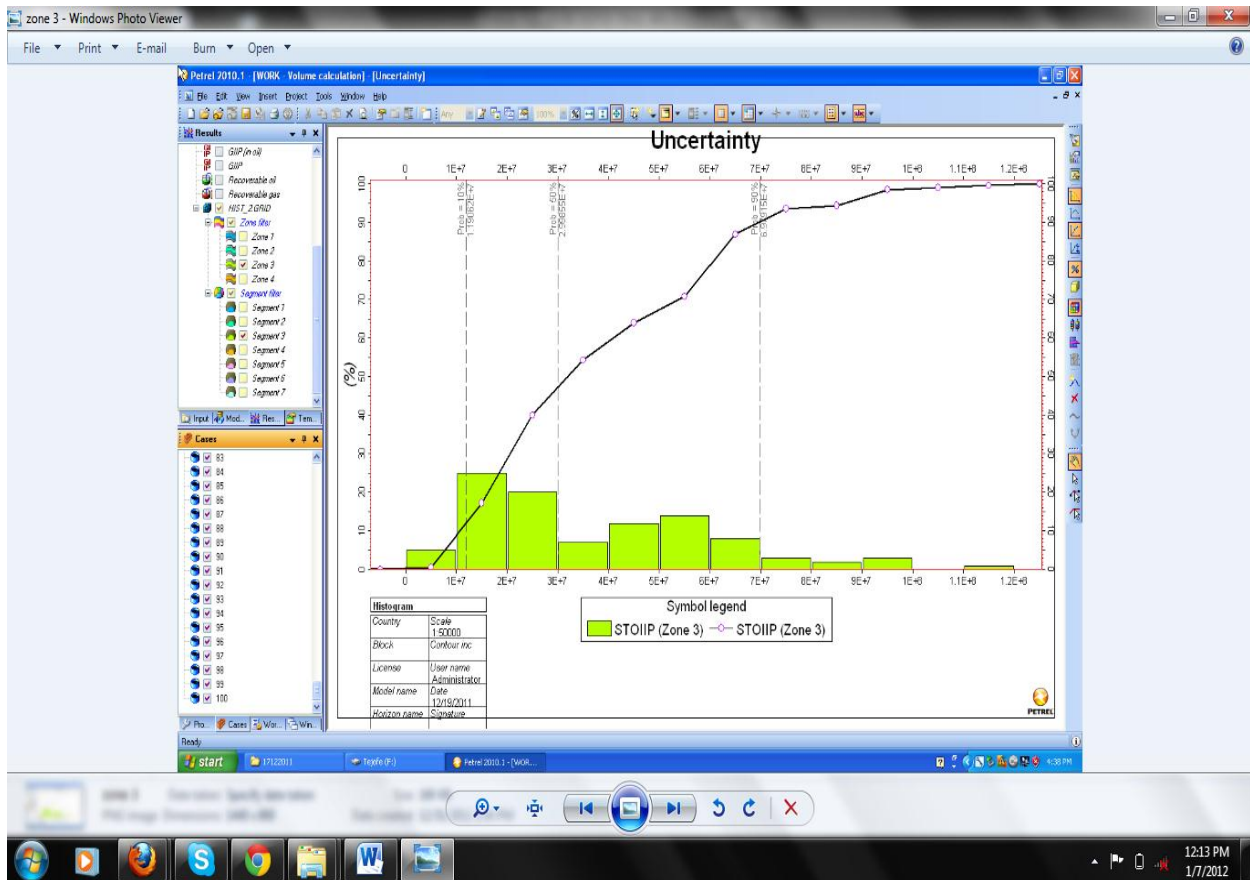


Figure 4.3: Histogram Plot of STOIP for Zone 3

A comparison of the STOIP in Zone2 vs. Zone 3 indicated that Zone 2 of this reservoir contains more oil in place than Zone 3.

4.4 Pertinent Remarks

The results of this study show that the volume of oil in place (STOIP) is gradually decreasing with reservoir depth. This is probably because the reservoir properties are degraded with increasing depth. Furthermore, the lower zones which are located close to the water leg (Zone 4) show noticeable decrease in STOIP.

CHAPTER FIVE

5.0 CONCLUSIONS AND RECOMMENDATION

5.1 Summary and Conclusions

A geologic model has been built for the OND Field. Using a Stochastic method (SGS), petrophysical parameters have been assigned to the grid blocks of the model in Fault block A of the G-1 sands in order to evaluate the uncertainty in STOOIP for the reservoir. Specifically, the following conclusions have been reached.

- The P10 STOOIP in Fault block A of the G-1 sands ranges from 17.9MMSTB in zone 1 to 14.9MMSTB in zone 2 and 11.9MMSTB in zone 3.
- The P50 STOOIP ranges from 45MMSTB in zone 1 to 37.5MMSTB in zone 2 and 30MMSTB in zone 3. Also, P90 STOOIP ranges from 104.7MMSTB in zone 1 to 87.2MMSTB in zone 2 and 69.8MMSTB in zone 3.
- These results show a general decline in STOOIP as the depth increases from Zone 1 to Zone 3 in Fault block A of the G-1 sands.
- This methodology has been validated using a case study with data from an offshore field (OND) in the Niger Delta.

5.2 Recommendation

This study used a grid cell-based methodology to evaluate uncertainty in the volume of oil in place in Fault Block A of the G-1 Sands.

- It is recommended that object-based conditional simulation be used to study uncertainty of STOOIP in the G-1 Sand. In object based conditional simulation modeling the reservoir attributes can be defined on a grid block scale and various objects with different

shapes and sizes can be simulated to honor the conditioning data.

- The proposed approach may provide additional information on the impact of reservoir properties on the uncertainty of estimates of the volume of fluids in place.
- This same methodology can be applied to the other sands of the OND field to quantify the uncertainties in the volume of oil in place for improved reservoir characterization.

REFERENCES

Akinwumi, F. V., Arochukwu, E. C., and Abdul-Kareem, A. S.: "Managing Uncertainties in Hydrocarbon-in-place Volumes in a Northern Depobelt Field, Niger Delta, Nigeria" paper SPE 88880, presented at the 28th Annual SPE International Technical Conference and Exhibition in Abuja, Nigeria, August 2-4, 2004.

Allen, J.R.L.: "Late Quaternary Niger Delta, and Adjacent Areas-Sedimentary Environments and Lithofacies," AAPG Bulletin, 1965, v.49, p.547-600.

Aprilia, A.W., Li, Z., McVay D.A., and Lee, W.J.: "Quantifying Uncertainty in Original-Gas-in-Place Estimates With Bayesian Integration of Volumetric and Material Balance Analyses," paper SPE 100575 presented at the 2006 SPE Gas Technology Symposium, Calgary, Alberta, Canada, May 15-17.

Baldwin, D.E.: "A Monte Carlo Model for Pressure Transient Analysis," paper SPE 2568 presented at 1969 SPE Annual Meeting, Denver, 28 September – 1 October.

Burke, K., 1972, Longshore drift, submarine canyons and submarine fans in development of Niger delta: AAPG Bulletin, v. 56:1975-1983.

Bustin, R. M.: "Sedimentology and Characteristics of Dispersed Organic Matter in Tertiary Niger Delta: Origin of Source Rocks in a Deltaic Environment," AAPG Bulletin, 1988, v. 72, p. 277-298.

Capen, E.C.: “The Difficulty of Assessing Uncertainty,” paper SPE 5579 presented at the 1975 SPE-AIME Annual Technical Conference and Exhibition, Dallas, 28 September – 1 October.

Doust, H. and E. Omatsola, 1989. Niger delta: AAPG Memoir 48 p. 201-238.

Efron, B.: “Why Isn’t Everyone a Bayesian,” American Statistician (1986) **40**, No.1, 1.

Ekweozor, C.M. and N.V. Okoye, 1980, Petroleum source-bed evaluation of Tertiary Niger Delta: AAPG Bulletin, v. 64, p. 1251-1259.

Evamy, B.D., J. Haremboure, R. Kammerling, W.A. Knaap, F.A. Molloy, and P.H. Rowlands, 1978. Hydrocarbon habitat of tertiary Niger Delta: AAPG Bulletin, v.62:1-39.

Ezekwe, J. N., and Filler, S. L.: “Modelling Deepwater Reservoirs,” paper SPE 95066 presented at the 2005 SPE Annual Technical Conference and Exhibition held in Dallas, Texas, U.S.A., 9 – 12 October 2005.

Fair, W.B.: “A Statistical Approach to Material Balance Methods,” paper SPE 28629 presented at the 1994 SPE Annual Technical Conference and Exhibition, New Orleans, Louisiana, 25–28 September.

Floris F.J.T., Bush M.D, Cuypers M., Roggero F., and Syversveen A-R.: “Methods for Quantifying the Uncertainty of Production Forecasts: A Comparative Study,” Petroleum Geoscience **7** (2001) S87-S96.

Galli A., Armstrong, M., and Dias, M.A.: “The Value of Information: A Bayesian Real Option Approach,” paper SPE 90418 presented at the 2004 SPE Annual Technical Conference and Exhibition, Houston, 26-29 September.

Galli, A., Armstrong, M. and Jehl, B: “Comparing Three Methods for Evaluating Oil Projects: Option Pricing, Decision Trees, and Monte Carlo Simulations,” paper SPE 52949 presented at the 1999 Hydrocarbon Economics and Evaluation Symposium, Dallas, 20-23 March.

Garb, F.A.: “Assessing Risk and Uncertainty in Evaluation Hydrocarbon Producing Properties,” paper 1986 SPE 15921 presented at the SPE Eastern Regional Meeting, Columbus, Ohio, 12 – 14 November.

Gilman, J.R., Brickey, R.T. and Redd, M.M.: “Monte Carlo Techniques for Evaluating Producing Properties,” paper SPE 39925 presented at the 1998 SPE Rocky Mountain Regional Low Permeability Reservoirs Symposium, Denver, 5 – 8 April.

Glimm J., Hou S., Lee Y., Sharp D., and Ye K.: “Prediction of Oil Production with Confidence Intervals,” paper SPE 66350 presented at the 2001 SPE Reservoir Simulation Symposium, Houston, 11-14 February.

Guohong Zhang : “Estimating Uncertainties in Integrated Reservoir Studies,” . PhD Dissertation, Unpublished, Texas A&M University, December, 2003.

Han, C., Kang, J.M, and Choe, J.: “Monte Carlo Simulation on the Effect of Fracture Characteristics on Reduction of Permeability by In-Situ Bacteria Growth,” paper SPE 72166 presented at the 2001 Asia Pacific Improve Oil Recovery Conference, Kuala Lumpur, 8 – 9 October.

Huffman, C.H. and Thompson, R.S.: “Probability Ranges for Reserves Estimates From Decline Curve Analysis,” paper SPE 28333 presented at the 1994 SPE Annual Technical Conference and Exhibition, New Orleans, 25 – 28 September.

Kelkar, M. and Perez, G.: Applied Geostatistics for Reservoir Characterization, SPE, Dallas, TX (2002).

Kokolis, G.P., Litvak, B.L., Rapp, W.J. and Wang, B.: “Scenario Selection for Valuation of Multiple Prospect Opportunities: A Monte Carlo Play Simulation Approach,” paper SPE 52977 presented at the 1999 Hydrocarbon Economics and Evaluation Symposium, Dallas, 20-23 March.

Komlosi, Z.P.: “Application: Monte Carlo Simulation in Risk Evaluation of E & P Projects,” paper SPE 68578 present at the 2001 SPE Hydrocarbon Economics and Evaluation Symposium, Dallas, 2-3 April.

Lambert-Aikhionbare, D.O. and A.C. Ibe, 1984, Petroleum source-bed evaluation of the Tertiary Niger Delta: discussion: AAPG Bulletin, v. 68, p. 387-394.

Lumley, D.E., Nunns, A.G., Delorme, G., Adeogba, A.A., and Bee, M.F.: “Meren Field, Nigeria: A 4D Seismic Case Study,” paper OTC 12098 presented at the 2000 Offshore Technology Conference, Houston, TX, May 1-4, 2000.

McEwen, C.R.: “Material Balance Calculations with Water Influx in the Presence of Uncertainty in Pressures,” *Trans.*, AIME (1962) **225**, 120.

Murtha, J.A.: “Monte Carlo Simulation: Its Status and Future,” paper SPE 37932 presented at the 1997 SPE Annual Technical Conference and Exhibition, San Antonio, 5 – 8 October.

Murtha, J.A.: “Incorporating Historical Data in Monte Carlo Simulation,” paper SPE 26245 presented at the 1993 SPE Petroleum Computer Conference, New Orleans, 11 – 14 July.

Murtha, J.A.: “Infill Drilling in the Clinton: Monte Carlo Techniques Applied to the Material Balance Equation,” paper SPE 17068 presented at the 1987 SPE Eastern Regional Meeting, Pittsburgh, 21 – 23 October.

Odai L.A and Ogbe D.D.: Building and Ranking of Geostatistical Petroleum Reservoir Models, MSc. Thesis, Unpublished, AUST, December, 2010.

Ogele, C., Daoud, A.M., McVay, D.A., and Lee, W.J.: “Integration of Volumetric and Material Balance Analyses Using a Bayesian Framework To Estimate OHIP and Quantify Uncertainty,” Paper SPE 100257 presented at the SPE Europec/EAGE Annual Conference and Exhibition, Vienna, Austria, 12–15 June 2006.

Owoyemi A.O.D.: The Sequence Stratigraphy of Niger Delta, Delta Field, Offshore Nigeria,” MSc. Thesis, Unpublished, Texas A & M University, August, 2004.

Peterson, S.K., Murtha, J.A. and Schneider, F.F.: “Brief: Risk Analysis and Monte Carlo Simulation Applied to the Generation of Drilling AFE Estimates,” JPT (June 1995) P504.

Poston, S.W., Berry, P., and Molokwu, F.W.: “Meren Field – The Geology and Reservoir Characteristics of a Nigerian Offshore Field,” paper SPE 10344 presented at the 1981 SPE Annual Technical Conference and Exhibition, San Antonio, Oct. 5-7.

Salomao, M.C. and Grell, A.P.: “Uncertainty in Production Profiles on the Basis of Geostatistic Characterization and Flow Simulation,” paper SPE 69477 presented at the 2001 SPE Latin American and Caribbean Petroleum Engineering Conference, Buenos Aires, Argentina, 25 – 28 March.

Scales, J.A. and Snieder, R.: “To Bayes or Not to Bayes,” Geophysics (July/August 1997) **62**, No. 4, 1045.

Short, K. C., and A. J. Stauble, 1967, Outline of Geology of Niger delta: American Association of Petroleum Geologists Bulletin v. 51, p. 761-779.

Thakur, G.D., et al.: “Engineering Studies of G-1, G-2, and G-3 Reservoirs, Meren Field, Nigeria,” paper SPE 10362, April 1982.

Vega, L., Rojas, D., and Datta-Gupta, A.: “Scalability of the Deterministic and Bayesian Approaches to Production-Data Integration Into Reservoir Models,” paper SPE 88961 presented at the 2003 SPE Reservoir Simulation Symposium, Houston, 3–5 February.

Verbruggen, R., Pannett, S., and Stone, G.: “Understanding Reserves Uncertainties in a Mature Field by Reservoir Modelling,” paper SPE 77896 presented at the 2002 SPE Asia Pacific Oil and Gas Conference and Exhibition (APOGCE), Melbourne, Australia, 8-10 October.

Wang, B. and Hwan, R.R.: “Influence of Reservoir Drive Mechanism on Uncertainties of Material Balance Calculations,” paper SPE 38918 presented at the 1997 SPE Annual Technical Conference and Exhibition, San Antonio, Texas, 5–8 October.

Weber, K.J., 1986, Hydrocarbon distribution patterns in Nigerian growth fault structures controlled by structural style and stratigraphy: AAPG Bulletin, v. 70 p. 661-662.

Weber, K.J. et al.: “The Role of Faults in Hydrocarbon Migration and Trapping in Nigerian Growth Fault Structures,” paper OTC 3054 presented at the 1978 Offshore Technology Conference, Houston.

Weber, K.J. and E.M. Daukoru, 1975, Petroleum geology of the Niger delta: Proceedings of the 9th World Petroleum Congress, Tokyo, v. 2, p. 202-221.

Whiteman, A. J., 1982, Nigeria, its petroleum, geology, resources and potential. v. I and II, Edinburgh, Graham and Trotman.

Wiggins, M.L. and Zhang, X.: "Using PC's and Monte Carlo Simulation To Assess Risks in Workover Evaluations," paper SPE 26243 presented at the 1993 SPE Petroleum Computer Conference, New Orleans, 11 – 14 July.

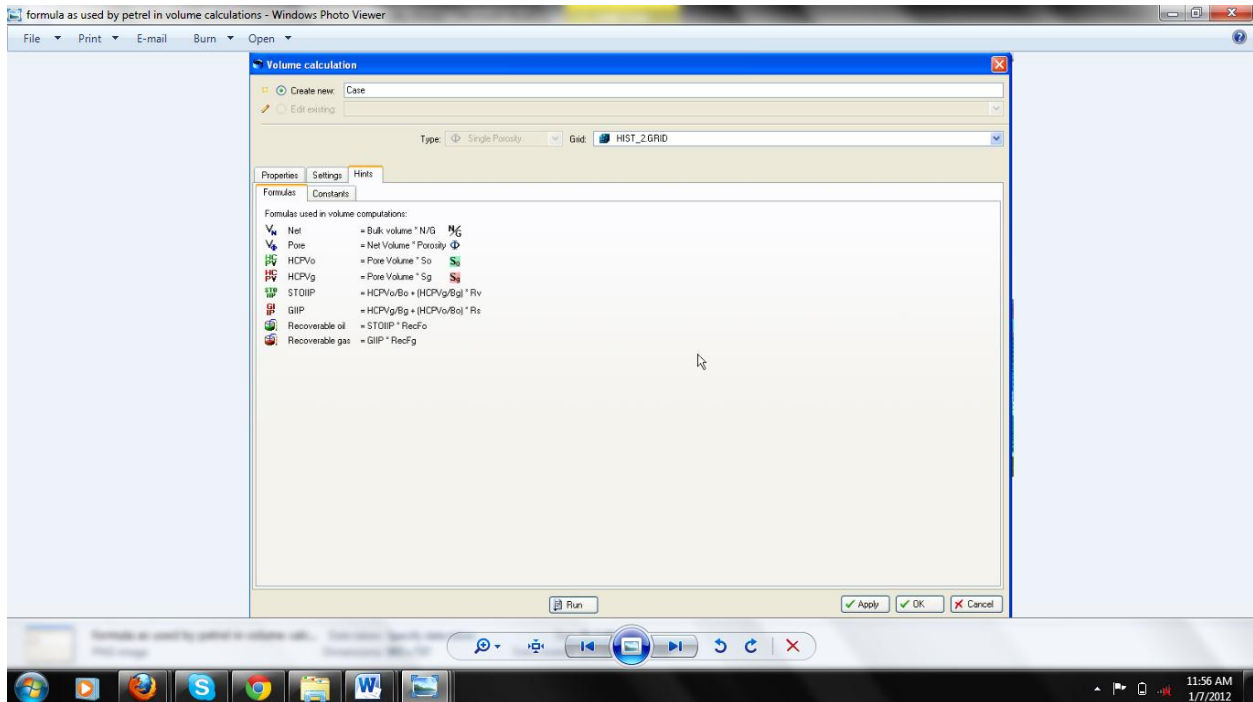
APPENDICES

APPENDIX A: NOMENCLATURE AND ABBREVIATIONS

Φ	Porosity
B	Formation Volume factor
OHIP	Original Hydrocarbon in Place
STOOIP	Stock Tank Original Hydrocarbon in Place
GRV	Gross Rock Volume
N/G	Net-to-Gross Ratio
PDF	Probability Density Function
A	Area
h	Thickness
Sw	Water Saturation

Subscripts

o	Oil
i	Initial
n	Total number of realizations
h	Horizontal



APPENDIX B: MODEL GRID FILE

RUNSPEC

FRONTSIM

TITLE
MEREN - OFFSHORE FIELD GRID FILE

DIMENS
110 60 4 /

FIELD

OIL

WATER

START
12 December 2011 /

UNIFOUT

GRID

GRIDFILE
2 /

INIT

DXV
110*380.98 / THAT IS SIZE OF EACH CELL IN THE X DIRECTION (ft)

DYV
60*380.98 / THAT IS SIZE OF EACH CELL IN THE Y DIRECTION (ft)

DEPTHZ
6771*6100 / THAT IS DEPTH FROM DATUM TO TOP OF MODEL

THICKZ
6771*30 THAT IS THICKNESS OF EACH ZONE
6771*25
6771*20
6771*63
/

PERMX
26400*1500 / THAT IS PERMEABILITY IS 1500 MD

COPY
PERMX PERMY /
PERMX PERMZ /
/

PORO
26400*0.27 /

PROPS

INCLUDE
'deadoil.inc' /

REGIONS

SOLUTION

EQUIL
2500 250 2600 1* 2000 1* 1 /

RPTSOL
RESTART=2 /

END

APPENDIX C: FAULT CODE FILE

-- Format : ECLIPSE fault data (ASCII)
-- Exported by: Petrel 2010.1 Schlumberger
-- User name : Enaworu Efeoghene
-- Date : Tuesday, October 25 2011 13:18:20
-- Project : Thesis Model
-- KEYWORD "FAULTS" HAS BEEN WRITTEN FROM PETREL.
FAULTS
-- Matrix Faults

-- NAME	IX1	IX2	IY1	IY2	IZ1	IZ2	FACE
'FAULT1'	1	5	20	20	1	3	'Y-'
'FAULT1'	5	5	21	21	1	3	'X+'
'FAULT1'	6	9	21	21	1	3	'Y-'
'FAULT1'	9	9	22	22	1	3	'X+'
'FAULT1'	10	13	22	22	1	3	'Y-'
'FAULT1'	13	13	23	23	1	3	'X+'
'FAULT1'	14	18	23	23	1	3	'Y-'
'FAULT1'	18	18	24	24	1	3	'X+'
'FAULT1'	19	24	24	24	1	3	'Y-'
'FAULT1'	24	24	25	25	1	3	'X+'
'FAULT1'	25	30	25	25	1	3	'Y-'
'FAULT1'	30	30	26	26	1	3	'X+'
'FAULT1'	31	34	26	26	1	3	'Y-'
'FAULT1'	34	34	27	27	1	3	'X+'
'FAULT1'	35	41	27	27	1	3	'Y-'
'FAULT1'	41	41	28	28	1	3	'X+'
'FAULT1'	42	46	28	28	1	3	'Y-'
'FAULT1'	46	46	28	28	1	3	'X-'
'FAULT1'	47	48	27	27	1	3	'Y-'
'FAULT1'	48	48	27	27	1	3	'X-'
'FAULT1'	49	50	26	26	1	3	'Y-'
'FAULT1'	50	50	26	26	1	3	'X-'
'FAULT1'	51	53	25	25	1	3	'Y-'
'FAULT1'	53	53	25	25	1	3	'X-'
'FAULT1'	54	55	24	24	1	3	'Y-'
'FAULT1'	55	55	24	24	1	3	'X-'
'FAULT1'	56	56	23	23	1	3	'Y-'
'FAULT1'	56	56	23	23	1	3	'X-'
'FAULT1'	57	58	22	22	1	3	'Y-'
'FAULT1'	58	58	22	22	1	3	'X-'
'FAULT1'	59	59	21	21	1	3	'Y-'
'FAULT1'	59	59	21	21	1	3	'X-'
'FAULT1'	60	60	20	20	1	3	'Y-'
'FAULT1'	60	60	20	20	1	3	'X-'

'FAULT1' 61 61 19 19 1 3 'Y-' /
 'FAULT1' 61 61 19 19 1 3 'X-' /
 'FAULT1' 62 62 18 18 1 3 'Y-' /
 'FAULT1' 62 62 18 18 1 3 'X-' /
 'FAULT1' 63 64 17 17 1 3 'Y-' /
 'FAULT1' 64 64 17 17 1 3 'X-' /
 'FAULT1' 65 66 16 16 1 3 'Y-' /
 'FAULT1' 66 66 16 16 1 3 'X-' /
 'FAULT1' 67 71 15 15 1 3 'Y-' /
 'FAULT1' 71 71 15 15 1 3 'X-' /
 'FAULT1' 72 77 14 14 1 3 'Y-' /
 'FAULT1' 77 77 15 15 1 3 'X+' /
 'FAULT1' 78 85 15 15 1 3 'Y-' /
 'FAULT1' 85 85 16 16 1 3 'X+' /
 'FAULT1' 86 89 16 16 1 3 'Y-' /
 'FAULT1' 89 89 17 17 1 3 'X+' /
 'FAULT1' 90 92 17 17 1 3 'Y-' /
 'FAULT1' 92 92 18 18 1 3 'X+' /
 'FAULT1' 93 94 18 18 1 3 'Y-' /
 'FAULT1' 94 94 19 19 1 3 'X+' /
 'FAULT1' 95 96 19 19 1 3 'Y-' /
 'FAULT1' 96 96 20 20 1 3 'X+' /
 'FAULT1' 97 98 20 20 1 3 'Y-' /
 'FAULT1' 98 98 21 21 1 3 'X+' /
 'FAULT1' 99 99 21 21 1 3 'Y-' /
 'FAULT1' 99 99 22 22 1 3 'X+' /
 'FAULT1' 100 101 22 22 1 3 'Y-' /
 'FAULT1' 101 101 23 23 1 3 'X+' /
 'FAULT1' 102 102 23 23 1 3 'Y-' /
 'FAULT1' 102 102 24 24 1 3 'X+' /
 'FAULT1' 103 104 24 24 1 3 'Y-' /
 'FAULT1' 104 104 25 25 1 3 'X+' /
 'FAULT1' 105 105 25 25 1 3 'Y-' /
 'FAULT1' 105 105 26 26 1 3 'X+' /
 'FAULT1' 106 107 26 26 1 3 'Y-' /
 'FAULT1' 107 107 27 27 1 3 'X+' /
 'FAULT1' 108 108 27 27 1 3 'Y-' /
 'FAULT1' 108 108 28 28 1 3 'X+' /
 'FAULT1' 109 110 28 28 1 3 'Y-' /

-- FAULT1

-- NAME IX1 IX2 IY1 IY2 IZ1 IZ2 FACE
 'FAULT2' 1 1 38 38 3 3 'Y-' /
 'FAULT2' 1 1 39 39 3 3 'X+' /
 'FAULT2' 2 2 39 39 3 3 'Y-' /

'FAULT2' 2 2 40 40 3 3 'X+' /
'FAULT2' 3 5 40 40 3 3 'Y-' /
'FAULT2' 5 5 41 41 3 3 'X+' /
'FAULT2' 6 8 41 41 3 3 'Y-' /
'FAULT2' 8 8 42 42 3 3 'X+' /
'FAULT2' 9 12 42 42 3 3 'Y-' /
'FAULT2' 12 12 43 43 3 3 'X+' /
'FAULT2' 13 18 43 43 3 3 'Y-' /
'FAULT2' 18 18 43 43 3 3 'X-' /
'FAULT2' 19 26 42 42 3 3 'Y-' /
'FAULT2' 26 26 43 43 3 3 'X+' /
'FAULT2' 27 30 43 43 3 3 'Y-' /
'FAULT2' 30 30 44 44 3 3 'X+' /
'FAULT2' 31 32 44 44 3 3 'Y-' /
'FAULT2' 32 32 45 45 3 3 'X+' /
'FAULT2' 33 44 45 45 3 3 'Y-' /
'FAULT2' 44 44 45 45 3 3 'X-' /
'FAULT2' 45 45 44 44 3 3 'Y-' /
'FAULT2' 45 45 44 44 3 3 'X-' /
'FAULT2' 46 47 43 43 3 3 'Y-' /
'FAULT2' 47 47 43 43 3 3 'X-' /
'FAULT2' 48 56 42 42 3 3 'Y-' /
'FAULT2' 56 56 43 43 3 3 'X-' /
'FAULT2' 57 62 43 43 3 3 'Y-' /
'FAULT2' 62 62 43 43 3 3 'X-' /
'FAULT2' 63 66 42 42 3 3 'Y-' /
'FAULT2' 66 66 42 42 3 3 'X-' /
'FAULT2' 67 70 41 41 3 3 'Y-' /
'FAULT2' 70 70 41 41 3 3 'X-' /
'FAULT2' 71 72 40 40 3 3 'Y-' /
'FAULT2' 72 72 40 40 3 3 'X-' /
'FAULT2' 73 79 39 39 3 3 'Y-' /
'FAULT2' 79 79 39 39 3 3 'X-' /
'FAULT2' 80 84 38 38 3 3 'Y-' /
'FAULT2' 84 84 38 38 3 3 'X-' /
'FAULT2' 85 88 37 37 3 3 'Y-' /
'FAULT2' 88 88 37 37 3 3 'X-' /
'FAULT2' 89 91 36 36 3 3 'Y-' /
'FAULT2' 91 91 36 36 3 3 'X-' /
'FAULT2' 92 95 35 35 3 3 'Y-' /
'FAULT2' 95 95 35 35 3 3 'X-' /
'FAULT2' 96 97 34 34 3 3 'Y-' /
'FAULT2' 97 97 34 34 3 3 'X-' /
'FAULT2' 98 99 33 33 3 3 'Y-' /
'FAULT2' 99 99 33 33 3 3 'X-' /
'FAULT2' 100 101 32 32 3 3 'Y-' /

'FAULT2' 101 101 32 32 3 3 'X-' /
'FAULT2' 102 103 31 31 3 3 'Y-' /
'FAULT2' 103 103 31 31 3 3 'X-' /
'FAULT2' 104 105 30 30 3 3 'Y-' /
'FAULT2' 105 105 30 30 3 3 'X-' /
'FAULT2' 106 107 29 29 3 3 'Y-' /
'FAULT2' 107 107 29 29 3 3 'X-' /
'FAULT2' 108 108 28 28 3 3 'Y-' /

-- FAULT2

-- NAME	IX1	IX2	IY1	IY2	IZ1	IZ2	FACE
'FAULT3'	30	35	59	59	1	3	'Y-' /
'FAULT3'	35	35	59	59	1	3	'X-' /
'FAULT3'	36	40	58	58	1	3	'Y-' /
'FAULT3'	40	40	58	58	1	3	'X-' /
'FAULT3'	41	45	57	57	1	3	'Y-' /
'FAULT3'	45	45	57	57	1	3	'X-' /
'FAULT3'	46	49	56	56	1	3	'Y-' /
'FAULT3'	49	49	56	56	1	3	'X-' /
'FAULT3'	50	53	55	55	1	3	'Y-' /
'FAULT3'	53	53	55	55	1	3	'X-' /
'FAULT3'	54	57	54	54	1	3	'Y-' /
'FAULT3'	57	57	54	54	1	3	'X-' /
'FAULT3'	58	68	53	53	1	3	'Y-' /
'FAULT3'	68	68	53	53	1	3	'X-' /
'FAULT3'	69	74	52	52	1	3	'Y-' /
'FAULT3'	74	74	52	52	1	3	'X-' /
'FAULT3'	75	78	51	51	1	3	'Y-' /
'FAULT3'	78	78	51	51	1	3	'X-' /
'FAULT3'	79	81	50	50	1	3	'Y-' /
'FAULT3'	81	81	50	50	1	3	'X-' /
'FAULT3'	82	83	49	49	1	3	'Y-' /
'FAULT3'	83	83	49	49	1	3	'X-' /
'FAULT3'	84	85	48	48	1	3	'Y-' /
'FAULT3'	85	85	48	48	1	3	'X-' /
'FAULT3'	86	87	47	47	1	3	'Y-' /
'FAULT3'	87	87	47	47	1	3	'X-' /
'FAULT3'	88	88	46	46	1	3	'Y-' /
'FAULT3'	88	88	46	46	1	3	'X-' /
'FAULT3'	89	90	45	45	1	3	'Y-' /
'FAULT3'	90	90	45	45	1	3	'X-' /
'FAULT3'	91	92	44	44	1	3	'Y-' /
'FAULT3'	92	92	44	44	1	3	'X-' /
'FAULT3'	93	93	43	43	1	3	'Y-' /
'FAULT3'	93	93	43	43	1	3	'X-' /

'FAULT3' 94 94 42 42 1 3 'Y-' /
 'FAULT3' 94 94 42 42 1 3 'X-' /
 'FAULT3' 95 95 41 41 1 3 'Y-' /
 'FAULT3' 95 95 41 41 1 3 'X-' /
 'FAULT3' 96 96 40 40 1 3 'Y-' /
 'FAULT3' 96 96 40 40 1 3 'X-' /
 'FAULT3' 97 97 39 39 1 3 'Y-' /
 'FAULT3' 97 97 39 39 1 3 'X-' /
 'FAULT3' 98 98 38 38 1 3 'Y-' /
 'FAULT3' 98 98 38 38 1 3 'X-' /
 'FAULT3' 99 99 37 37 1 3 'Y-' /
 'FAULT3' 99 99 37 37 1 3 'X-' /
 'FAULT3' 100 100 36 36 1 3 'Y-' /
 'FAULT3' 100 100 35 36 1 3 'X-' /
 'FAULT3' 101 101 34 34 1 3 'Y-' /
 'FAULT3' 101 101 34 34 1 3 'X-' /
 'FAULT3' 102 102 33 33 1 3 'Y-' /
 'FAULT3' 102 102 33 33 1 3 'X-' /
 'FAULT3' 103 103 32 32 1 3 'Y-' /
 'FAULT3' 103 103 32 32 1 3 'X-' /

-- FAULT3

-- NAME IX1 IX2 IY1 IY2 IZ1 IZ2 FACE
 'FAULT4' 46 46 29 29 1 3 'X+' /
 'FAULT4' 47 48 29 29 1 3 'Y-' /
 'FAULT4' 48 48 30 30 1 3 'X+' /
 'FAULT4' 49 50 30 30 1 3 'Y-' /
 'FAULT4' 50 50 31 31 1 3 'X+' /
 'FAULT4' 51 52 31 31 1 3 'Y-' /
 'FAULT4' 52 52 32 32 1 3 'X+' /
 'FAULT4' 53 53 32 32 1 3 'Y-' /
 'FAULT4' 53 53 33 33 1 3 'X+' /
 'FAULT4' 54 54 33 33 1 3 'Y-' /
 'FAULT4' 54 54 34 34 1 3 'X+' /
 'FAULT4' 55 55 34 34 1 3 'Y-' /
 'FAULT4' 55 55 35 35 1 3 'X+' /
 'FAULT4' 56 57 35 35 1 3 'Y-' /
 'FAULT4' 57 57 36 36 1 3 'X+' /
 'FAULT4' 58 58 36 36 1 3 'Y-' /
 'FAULT4' 58 58 37 37 1 3 'X+' /
 'FAULT4' 59 59 37 37 1 3 'Y-' /
 'FAULT4' 59 59 38 38 1 3 'X+' /
 'FAULT4' 60 61 38 38 1 3 'Y-' /
 'FAULT4' 61 61 39 39 1 3 'X+' /
 'FAULT4' 62 62 39 39 1 3 'Y-' /

'FAULT4' 62 62 40 40 1 3 'X+' /
'FAULT4' 63 64 40 40 1 3 'Y-' /
'FAULT4' 64 64 41 41 1 3 'X+' /
'FAULT4' 65 66 41 41 1 3 'Y-' /

-- FAULT4

-- NAME IX1 IX2 IY1 IY2 IZ1 IZ2 FACE
'FAULT5' 1 13 50 50 1 3 'Y-' /
'FAULT5' 13 13 51 51 1 3 'X+' /
'FAULT5' 14 16 51 51 1 3 'Y-' /
'FAULT5' 16 16 52 52 1 3 'X+' /
'FAULT5' 17 19 52 52 1 3 'Y-' /
'FAULT5' 19 19 53 53 1 3 'X+' /
'FAULT5' 20 21 53 53 1 3 'Y-' /
'FAULT5' 21 21 54 54 1 3 'X+' /
'FAULT5' 22 23 54 54 1 3 'Y-' /
'FAULT5' 23 23 55 55 1 3 'X+' /
'FAULT5' 24 24 55 55 1 3 'Y-' /
'FAULT5' 24 24 56 56 1 2 'X+' /
'FAULT5' 25 26 56 56 1 3 'Y-' /
'FAULT5' 26 26 57 57 1 3 'X+' /
'FAULT5' 27 27 57 57 1 3 'Y-' /
'FAULT5' 27 27 58 58 1 3 'X+' /
'FAULT5' 28 29 58 58 1 3 'Y-' /
'FAULT5' 29 29 59 59 1 2 'X+' /

-- FAULT5

-- NAME IX1 IX2 IY1 IY2 IZ1 IZ2 FACE
'FAULT6' 84 84 15 15 1 3 'X-' /
'FAULT6' 85 85 14 14 1 3 'Y-' /
'FAULT6' 85 85 14 14 1 3 'X-' /
'FAULT6' 86 86 13 13 1 3 'Y-' /
'FAULT6' 86 86 13 13 1 3 'X-' /
'FAULT6' 87 88 12 12 1 3 'Y-' /
'FAULT6' 88 88 12 12 1 3 'X-' /
'FAULT6' 89 90 11 11 1 3 'Y-' /
'FAULT6' 90 90 11 11 1 3 'X-' /
'FAULT6' 91 93 10 10 1 3 'Y-' /
'FAULT6' 93 93 10 10 1 3 'X-' /
'FAULT6' 94 95 9 9 1 3 'Y-' /
'FAULT6' 95 95 9 9 1 3 'X-' /
'FAULT6' 96 97 8 8 1 3 'Y-' /
'FAULT6' 97 97 8 8 1 3 'X-' /
'FAULT6' 98 99 7 7 1 3 'Y-' /

'FAULT6' 99 99 7 7 1 3 'X-' /
'FAULT6' 100 102 6 6 1 3 'Y-' /
'FAULT6' 102 102 6 6 1 3 'X-' /
'FAULT6' 103 105 5 5 1 3 'Y-' /
'FAULT6' 105 105 5 5 1 3 'X-' /
'FAULT6' 106 107 4 4 1 3 'Y-' /
'FAULT6' 107 107 4 4 1 3 'X-' /
'FAULT6' 108 110 3 3 1 3 'Y-' /

-- FAULT6

/

APPENDIX D: ADDITIONAL FIGURES FOR CHAPTER THREE

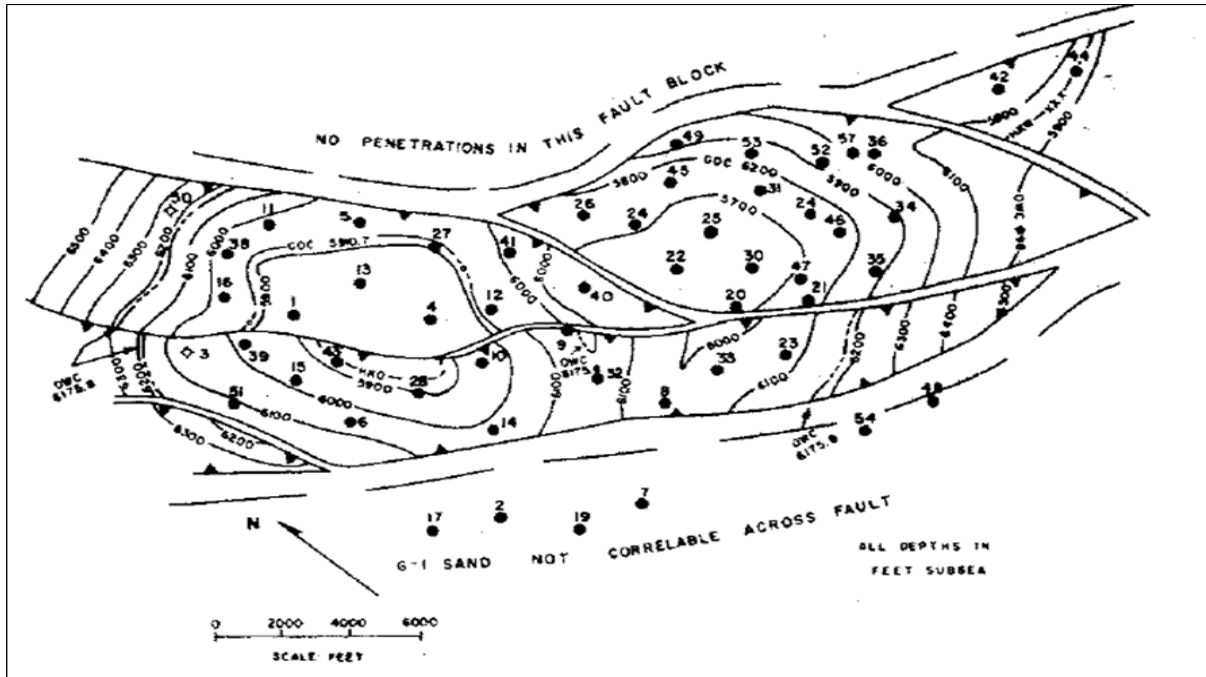


Figure D1: G-1 Sands Isopach Map

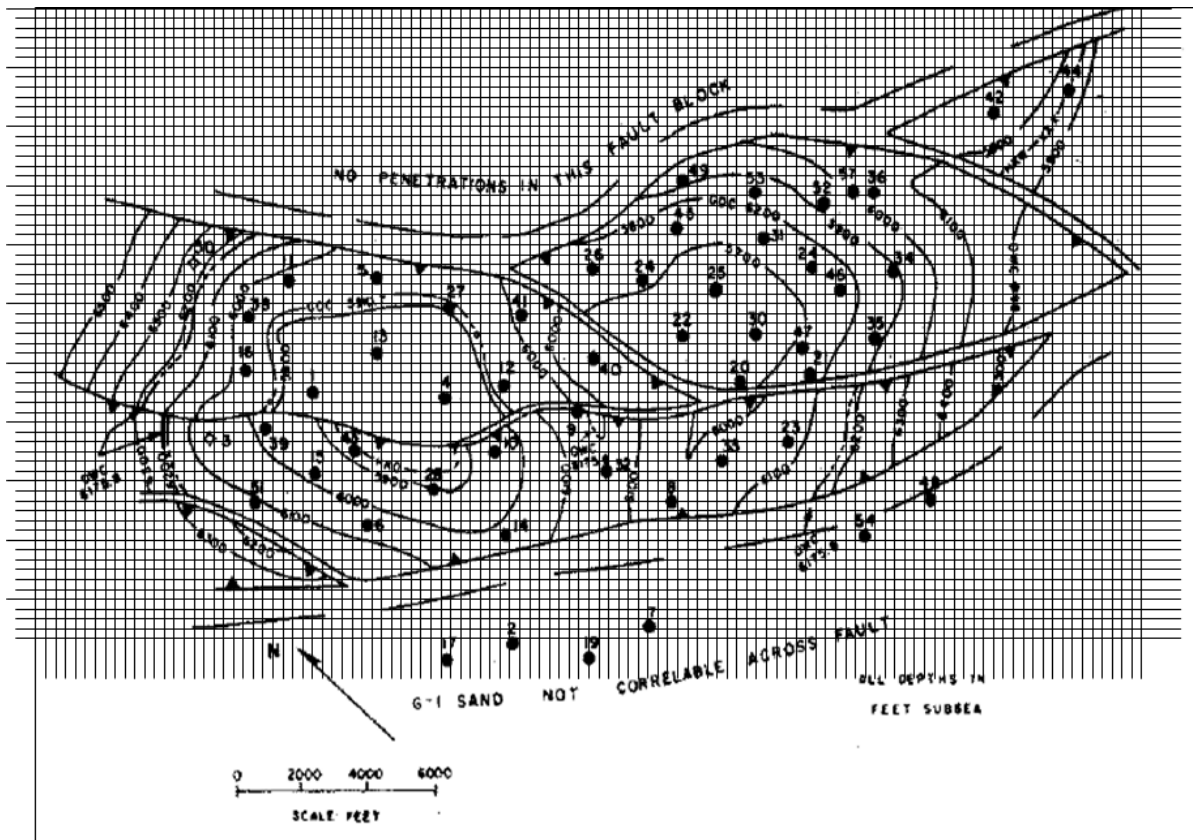


Figure D2: G-1 Sands Gridded Isopach Map

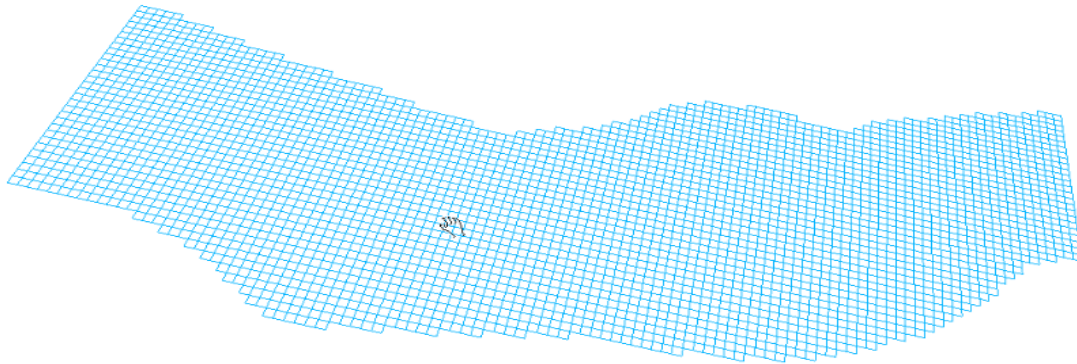


Figure D3a: Model Showing Areal View of Grid Cells.

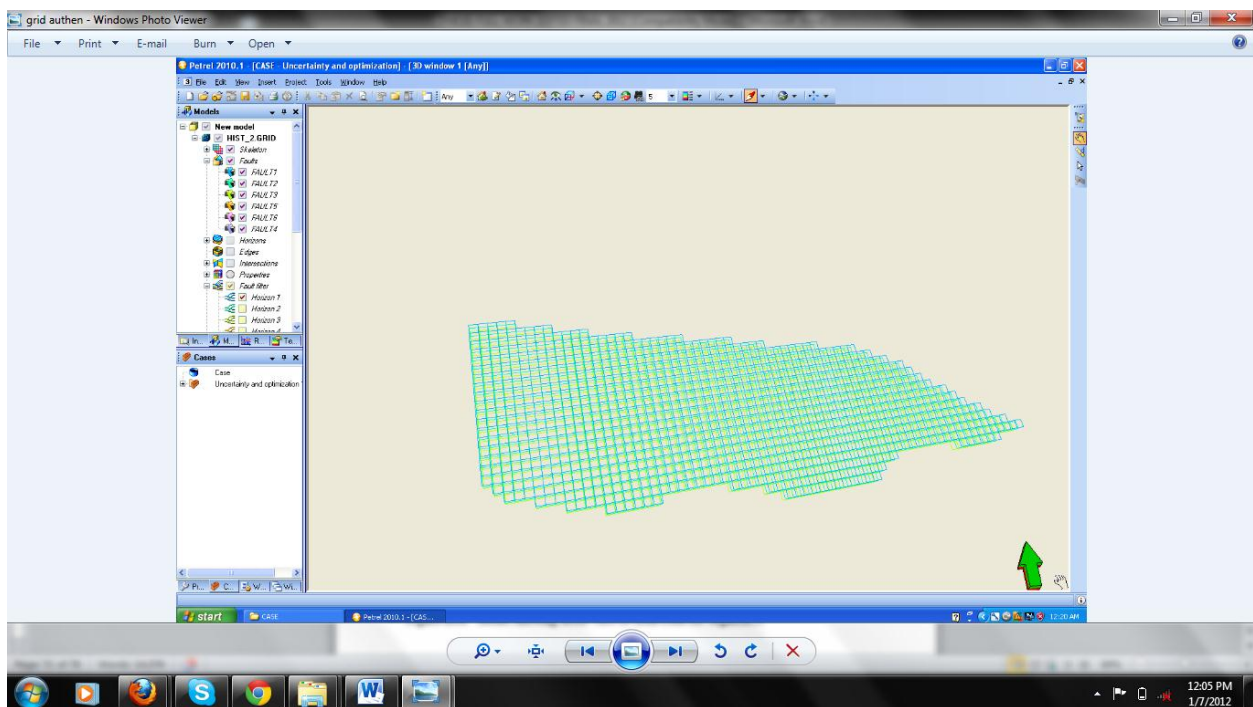


Figure D3b: Model Showing Areal View of Grid Cells for Segment 3.

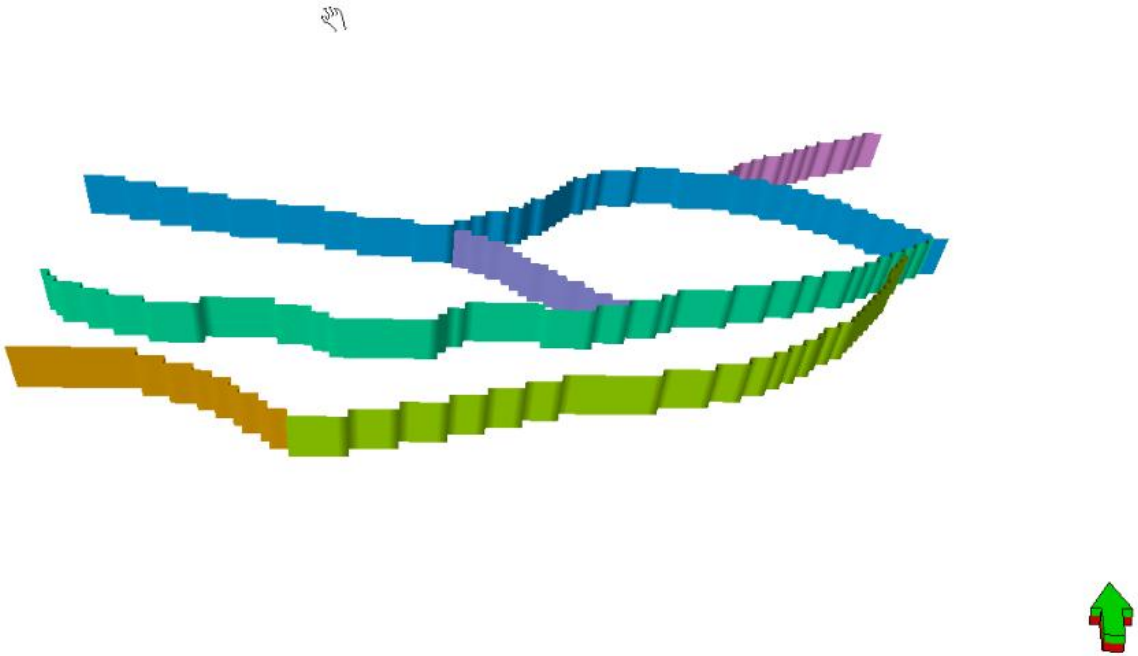


Figure D4: Grid Model Showing Fault Zones

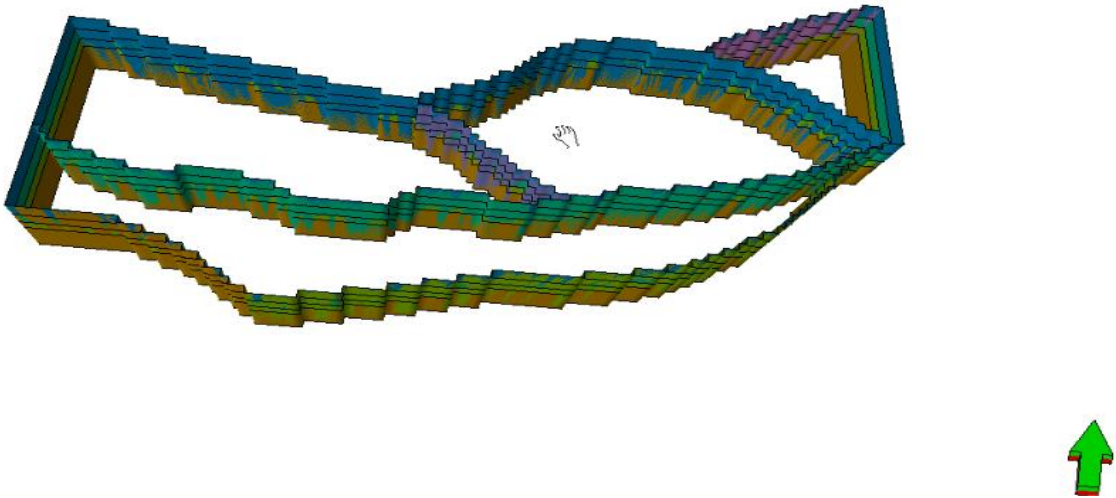


Figure D5: 3D Grid Model Showing Segments

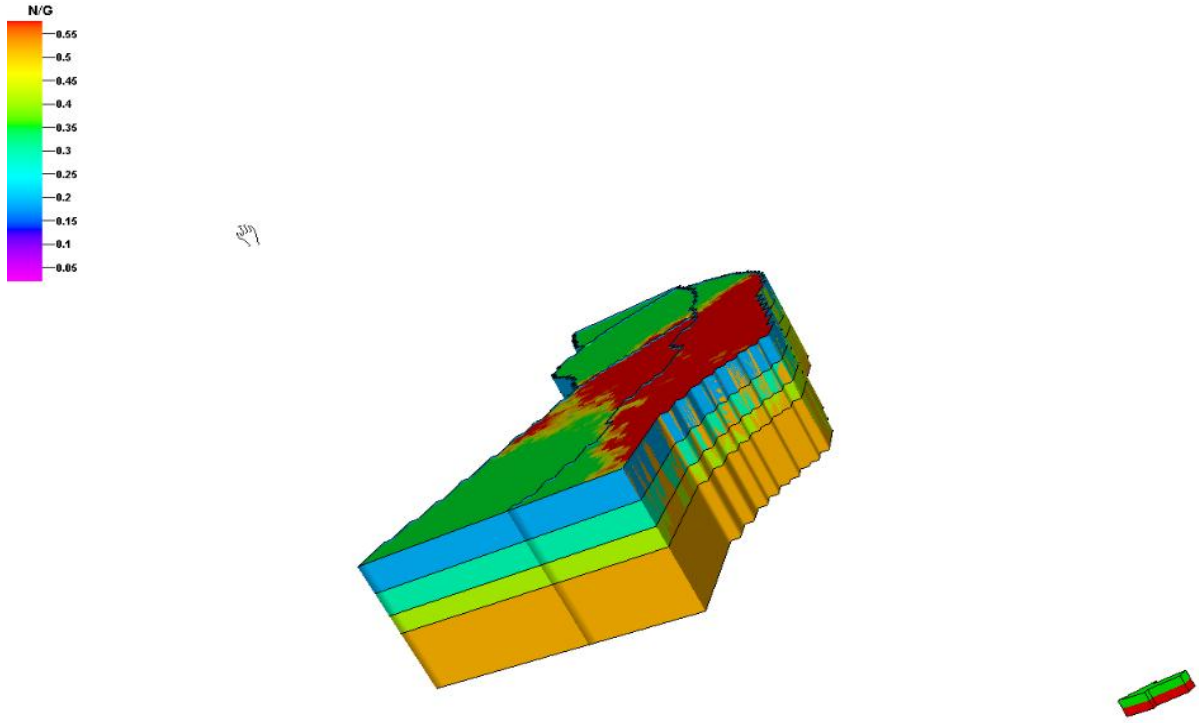


Figure D6: 3D Grid Model Showing Grid Zones


APPENDIX E: ADDITIONAL FIGURES AND TABLES FOR CHAPTER FOUR

Table E1: Variables of Some Parameters for STOOIP

Case name	\$ACCEPTED	\$LOOP	\$NG	\$Poro	\$Sw	STOOIP[*10 ⁶ STB]
1	True	1	0.9035504776146	0.2651706164385	0.6968162999359	106.6069
2	True	2	0.3040913144322	0.2127029795931	0.2148247566148	74.2352
3	True	3	0.8029941434980	0.1892957495614	0.4917593005157	112.9846
4	True	4	0.4783803827021	0.4536287861010	0.8566909024323	45.6948
5	True	5	0.3310538956877	0.4233814521483	0.2966758934293	144.2453
6	True	6	0.6513489181188	0.3400619278476	0.3323734488967	216.6778
7	True	7	0.4150367107150	0.2810748531749	0.7039881557664	50.5853
8	True	8	0.8849587817011	0.3892739450687	0.5594345561082	222.5556
9	True	9	0.5500993621631	0.2432307600293	0.6107803521835	76.1898
10	True	10	0.4014656086916	0.3602975490198	0.4105700094607	124.6064
11	True	11	0.4526882168034	0.3248168260533	0.7799820734275	47.4660
12	True	12	0.4189130252998	0.4088740736400	0.5862223578600	103.9718
13	True	13	0.8626910306100	0.3186355115037	0.4196101107821	233.9955
14	True	14	0.8775420239875	0.2953426207024	0.4495542619098	208.5270
15	True	15	0.7895005340739	0.2748571250911	0.5041774895474	157.3394
16	True	16	0.7240114963225	0.2355882822753	0.6651892117069	83.8829
17	True	17	0.3237929654835	0.2890810324675	0.2659610278633	100.7203
18	True	18	0.7460305551316	0.2932681512695	0.4982095065157	160.8008
19	True	19	0.3555167088839	0.2707025757448	0.6285341593676	52.4531
20	True	20	0.6084055940427	0.2129851730804	0.8962209723197	19.7376
21	True	21	0.4331939848017	0.2560446349702	0.3202595446638	110.4625
22	True	22	0.5094974517044	0.3575943364757	0.3962772576067	161.2931
23	True	23	0.9469358043153	0.3468603507312	0.2824469466231	345.7657
24	True	24	0.3648926816614	0.3210165604192	0.7478674977874	43.2690
25	True	25	0.4650682912686	0.4265321106312	0.3710721579638	183.3156
26	True	26	0.8721861903744	0.4257316904723	0.3789679799798	337.2679
27	True	27	0.7961733207190	0.2575147639886	0.4270584551530	171.5480
28	True	28	0.3917775597399	0.2206923845722	0.4071538071840	75.2955
29	True	29	0.9602390514847	0.3033142099778	0.5815207892086	178.1838
30	True	30	0.7053789483321	0.4570482979041	0.2463749839777	356.0039
31	True	31	0.9259365733817	0.2312864777212	0.8758673726615	39.1842
32	True	32	0.7412352793969	0.2712325356115	0.8818930539872	35.0197
33	True	33	0.6777334635456	0.2603093272027	0.5494217963194	64.9561
34	True	34	0.8234768272957	0.2874407617850	0.3122710684530	238.1487
35	True	35	0.9512743369853	0.3018988640509	0.4682303994872	223.9119
36	True	36	0.3849588427381	0.3217887045615	0.7600464705343	43.6019
37	True	37	0.9767500289925	0.2349284023794	0.8902911038544	37.0491
38	True	38	0.7190155400250	0.2321887407023	0.7188458876308	68.6912
39	True	39	0.5346646473586	0.2406872316207	0.8409752769554	30.0432
40	True	40	0.6604747245704	0.3968116028603	0.5145225409710	186.2320

41	True	41	0.7288775261696	0.4123806425103	0.4790008178960	229.3192
42	True	42	0.3727097476119	0.2366666992703	0.3211109103671	89.0775
43	True	43	0.7757586535233	0.2506225611651	0.6687656636249	94.4803
44	True	44	0.5330498001037	0.2428460452881	0.5337939817499	88.0087
45	True	45	0.8357907803582	0.3214352344396	0.4311196569719	223.7699
46	True	46	0.9079835596789	0.2300040613701	0.6917681203650	94.2633
47	True	47	0.6573259559923	0.2222540951530	0.7094103213599	62.1999
48	True	48	0.6720175420392	0.3391926676291	0.3553443189794	215.3311
49	True	49	0.7562235694448	0.2282359479568	0.6310768852809	93.2097
50	True	50	0.5238129459517	0.3246295822944	0.7902338389233	52.4097
51	True	51	0.3392356822412	0.2103582517623	0.4849925962096	53.7284
52	True	52	0.9162897976622	0.2595524187784	0.2869170903653	220.8410
53	True	53	0.8977955992309	0.3279824034839	0.5451424359874	261.1474
54	True	54	0.9759184575945	0.3442456779327	0.8159818079165	425.1047
55	True	55	0.8458488143559	0.2344741096564	0.5067743339335	211.7610
56	True	56	0.8408042148061	0.2418401103775	0.2588782464064	221.5796
57	True	57	0.7649412762840	0.2493403933103	0.8024349223303	128.9502
58	True	58	0.6995379436628	0.1988518052485	0.8182111941892	340.3709
59	True	59	0.5788324808496	0.3340503759178	0.8605438428907	214.7212
60	True	60	0.5020743766594	0.2289682281552	0.6418494094668	100.2384
61	True	61	0.6348764763328	0.3995197572702	0.4541292733542	221.5796
62	True	62	0.4879096560563	0.2728144423795	0.3529494186223	142.8837
63	True	63	0.4970316721091	0.2095997016777	0.5722172551652	131.8926
64	True	64	0.4833870784630	0.2684180297786	0.6799416547135	62.6934
65	True	65	0.5644249641407	0.3341365147437	0.8034833887752	56.6772
66	True	66	0.6884861934263	0.2210108896596	0.7902404980620	55.2512
67	True	67	0.7071675954466	0.2756831617051	0.8679728141117	62.4292
68	True	68	0.5947260444959	0.3248613210158	0.6755003601184	94.3032
69	True	69	0.6833514664143	0.4225424556437	0.8511217535935	64.9351
70	True	70	0.3538613574633	0.303396236854	0.7858005462813	39.9781
71	True	71	0.3152133976256	0.2487075110339	0.7706854884487	26.9647
72	True	72	0.438082125309	0.3196391885991	0.4589664540543	77.3770
73	True	73	0.4492947569200	0.1905827839563	0.5911218595638	42.9003
74	True	74	0.8151430036317	0.2044654261860	0.8310574877163	103.4654
75	True	75	0.6441046235541	0.3604468195249	0.8253948759422	68.5842
76	True	76	0.5157208655049	0.2814845011261	0.3419046174504	224.4877
77	True	77	0.9675976897488	0.2629871321490	0.3836461745048	264.4008
78	True	78	0.5570113650929	0.3403341183638	0.7212113071077	78.1273
79	True	79	0.8526628986480	0.2136854080256	0.4383258369701	151.9447
80	True	80	0.4271428235724	0.1967387010633	0.3823161259804	79.3288

81	True	81	0.9377263985106	0.2074254412591	0.6097864253669	113.1102
82	True	82	0.8041611651966	0.2885008709680	0.5239183080538	162.0835
83	True	83	0.3783652333140	0.2552514264387	0.568039332920	63.7071
84	True	84	0.987099237037	0.2141149704613	0.7341660481582	83.5743
85	True	85	0.4061018982512	0.3182861858542	0.6226588305307	73.0627
86	True	86	0.7820098635822	0.2139661954085	0.2315614734336	188.8380
87	True	87	0.5737689291055	0.4256479878539	0.5372792535172	165.9130
88	True	88	0.9310982543412	0.3796606156276	0.6568916074098	181.2645
89	True	89	0.3119248054445	0.1924041068329	0.2444446180608	66.3675
90	True	90	0.6188275063325	0.2669568016441	0.6508760338145	323.1370
91	True	91	0.5890962492751	0.3285142999174	0.7634070802941	68.4787
92	True	92	0.4695889736625	0.2330043284041	0.2180295388653	231.6067
93	True	93	0.8870329721976	0.3332704594441	0.7401641438032	111.9065
94	True	94	0.5973601611377	0.3116114405701	0.2774215094454	263.1698
95	True	95	0.3414269539475	0.2627482203054	0.3410113467818	151.2721
96	True	96	0.6261589800714	0.2913064051033	0.3013469283120	258.5096
97	True	97	0.7491662678914	0.2829884992306	0.4006191595202	250.5960
98	True	98	0.6154687917722	0.3086203794244	0.2253637501144	280.0911
99	True	99	0.5464732139042	0.3472793566165	0.2556724112674	262.2887
100	True	100	0.8278170445875	0.2231020601899	0.6005279549546	205.0425

Reset 

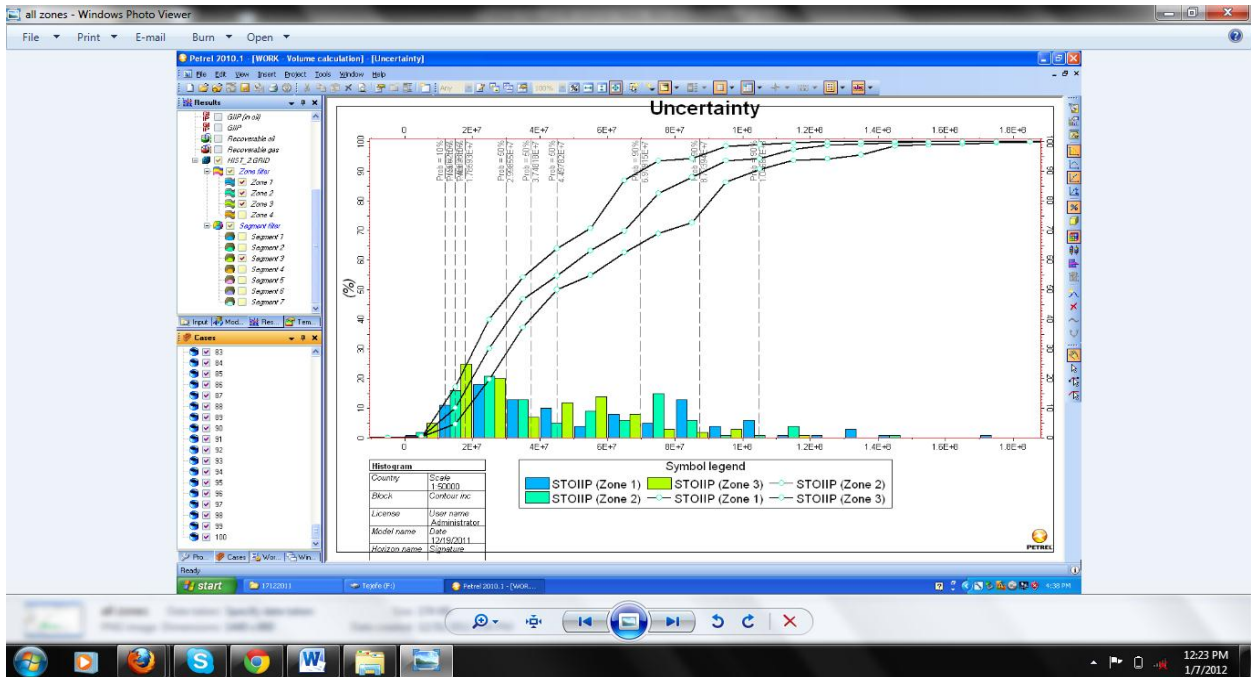


Figure E1: Uncertainty Evaluation of STOIP for all Zones.